THERMAL AND TRACTION BEHAVIOR IN SLIDING ELASTOHYDRODYNAMIC CONTACTS

A THESIS

Presented to

The Faculty of the Division of Graduate

Studies and Research

by

Richard K. Kunz

In Partial Fulfillment

of the Requirements for the Degree

Master of Science in Mechanical Engineering

Georgia Institute of Technology

November, 1974

THERMAL AND TRACTION BEHAVIOR IN SLIDING

ELASTOHYDRODYNAMIC CONTACTS

Approved:

Ward O. Winer, Chairman

George M. Rentzepis

David M. Sanborn

Date approved by Chairman: 19 Nov. 74

ACKNOWLEDGMENTS

The author wishes to thank the members of his reading committee for their time, interest, and valuable suggestions. The advice and assistance of the committee chairman, Professor Ward O. Winer, is particularly appreciated.

This research was supported in part by the National Science Foundation (NSF GK-31154) and NASA (NGR-11-002-133). The author is also grateful to the Georgia Tech Foundation and E. I. DuPont de Nemours and Company for fellowship support.

TABLE OF CONTENTS

TABLE OF CONTENTS (Continued)

LIST OF TABLES

LIST OF ILLUSTRATIONS

SUMMARY

An existing shear stress theory and lubricant rheological model were studied and evaluated by applying them to traction prediction in a sliding elastohydrodynamic point contact. A computer program was written to calculate shear stresses in the contact based on the theory, and to numerically integrate over the contact area to yield the traction. The results of such calculations, using measured film thicknesses and moving surface temperatures, were compared with measured tractions under several conditions of normal load and sliding speed. The comparison showed that the theory gives a relatively good traction prediction for high speeds, but that it appears to break down at lower speeds, where calculated tractions significantly exceed the measured values. Possible explanations for this disparity include the occurrence of asperity interactions at low speeds and thin films, and the onset of non-Newtonian lubricant behavior at the higher shear stresses which occur in the low speed range.

The effect on the traction of variations in the lubricant material properties was studied by varying the input parameters to the computer program. The traction was found to be increased by an increase in the inlet viscosity of the lubricant, and by a decrease in its temperature-viscosity dependence. A weaker increase in traction was obtained by

increasing the fluid's pressure-viscosity dependence.

In order to make the theory applicable to engineering use, a formula for calculating the film thickness was applied, as well as an iterative method for determining the temperature of the moving surface. The film thickness calculation was found to yield satisfactory results for most hydrocarbon oils. The method for determining the temperature is adequate for use in traction calculations at high speeds, but becomes less satisfactory as the speed decreases.

CHAPTER I

INTRODUCTION

The determination of the traction force in elastohydrodynamic contacts is of primary importance in the understanding of many lubricated mechanisms. However, due to the physical complexity of the problem, no simple model describing quantitatively the generation of traction in an EHD contact has yet been generally accepted. It is the purpose of this thesis to evaluate the theory of maximum film temperature and shear stress, as well as the rheological model of the lubricant, proposed by Jakobsen 1973 (1) and Jakobsen and Winer 1974 (2). This evaluation is performed by applying the theory to elastohydrodynamic point contacts in pure sliding, and comparing the results of these calculations with experimental data.

The phenomenon of elastohydrodynamic lubrication (EHD) arises in practice in gears, cams, and rolling element bearings. It occurs in cases where load is sufficiently high, and is carried over a sufficiently small surface area, that the hydrodynamic pressures generated cause significant elastic deformation of the bearing material. This deformation has the effect of enlarging the contact area between bearing surfaces, allowing for the formation of a full (al-

though thin) hydrodynamic film which carries the load. The presence of this film is responsible for the relatively long life of the above-mentioned components, and is therefore highly desirable.

In view of the above, the study of elastohydrodynamic lubrication necessitates a combination of the fields of elasticity, fluid mechanics, and lubricant rheology. Much of the early EHD research was devoted to the prediction of film thickness, primarily because of its great importance in the life of bearing elements. However, in recent years, more attention has been paid to an analytical representation of the generation of traction, or frictional resistance to the bearing motion due to viscous shearing of the lubricant. The traction force is directly related to the power loss in mechanical components. Furthermore, traction studies are in part motivated by a desire to predict the onset of skidding in rolling element bearings, according to Cheng 1974 (3).

Theoretical analyses of the generation of traction force have not met with the same degree of success as have the film thickness studies, due to complications caused by the larger role of thermal effects in the former, and by difficulties in finding a rheological model which is adequate at high pressures. Models proposed by Crook 1961 (4), Kannel and Walowit 1971 (5), and Allen, Townsend and Zaretsky 1970 (6) all assumed isothermal bearing surfaces, a condition which, based on experimental temperature measurements by

Turchina, Sanborn and Winer 1974 (7), appears to be violated physically, particularly when a great deal of sliding is present. Cheng and Sternlicht 1965 (8) and Cheng 1965 (9) included thermal effects in a numerical analysis dealing primarily with line contacts in the prediction of film thickness, pressure, and temperature. While these investigations give a great deal of insight into the effects of thermal behavior in the analysis, the complexity of the numerical iteration technique limits the usefulness of this model for the prediction of traction for a wide range of physical situations.

Archard and Baglin 1974 (14,15), in an attempt to develop a general model for traction, used physical reasoning in forming non-dimensional groups, much as was done in previous film-thickness investigations. As a result of assuming isothermal conditions, a Newtonian fluid, and an exponential pressure-viscosity relation, the immediate value of their theory is limited to low sliding speeds where thermal effects are less important. However, the model is significant in that it systematizes and generalizes traction studies to include rolling and sliding, flooded and starved conditions, and forms a foundation on which further solutions based on thermal effects and different rheological models may be built.

The theory advanced by Jakobsen 1973 (1) and Jakobsen and Winer 1974 (2) takes thermal effects into account, while

limiting to a few graphical steps the work required to find the shear stress at a point in the sliding EHD contact. The method is thus suitable for predicting tractions while eliminating the restrictions imposed by the assumption of isothermal walls. The present work seeks to replace the need for the dimensionless charts of Jakobsen 1974 (1) by the use of a computer program, facilitating the computation of tractions over the EHD contact. By comparing the calculations with experimental measurements, an evaluation of the model is possible.

Another primary difficulty in the development of a realistic model to predict traction has been the lack of an adequate description of the behavior of the lubricant under the extreme physical conditions of pressure, shear stress, and temperature gradients, as well as the short time of exposure, in the EHD contact. Such conditions are difficult to duplicate in viscometric measurements. Consequently, numerous fluid rheological models have been proposed for EHD analysis. Smith 1962 (10), in order to explain his experimental results, suggested that, at high shear stress, a phenomenon of yield occurs in the fluid, analogous to the yield stress of a plastic solid. Crook 1963 (11) attributed viscoelastic properties to the lubricant in order to account for the results of his measurements, and Dyson 1970 (12) employed a similar viscoelastic model in a theoretical development. Indeed, there seem to be nearly as many different

rheological models as there are investigators, whether to explain experimental results or to support a theoretical development.

Jakobsen 1973 (1) proposed a Newtonian model employing a power-exponential temperature-viscosity function which contains two material parameters, each of which is a function of pressure. His expression of the variation of viscosity with pressure and temperature resulted from the correlation of measurements on a capillary viscometer at shear stress levels only 3-5 times less than the average shear expected in an elastohydrodynamic contact. Previous investigations attained continuous shear stress levels three orders of magnitude less than this average value. The present work applies the Newtonian viscosity model to the EHD situation of a point contact in pure sliding.

Therefore, by applying both the theory and the rheological model of Jakobsen to the calculation of traction in an elastohydrodynamic point contact, this thesis attempts to evaluate the theory and the model as applied to elastohydrodynamic lubrication. Furthermore, a means for calculating the surface temperature, to be used in place of a measured temperature distribution, is presented and evaluated for use in traction calculations. The effect on such computations of using calculated rather than measured film thickness is also explored.

While the terminology of this thesis is consistent

with the literature in the field, some clarification of terms is warranted. "Traction" and "traction force" refer to that force, arising in the contact area, which resists the relative motion of the bearing surfaces. The "traction coefficient" is the ratio between the traction force and the normal load. It is therefore analogous to the coefficient of friction in ordinary sliding. The "sliding speed" is the relative velocity between the bearing surfaces. Furthermore, a "point contact" is not in fact a point, but a region. Due to the geometry of the bearing surfaces, the contact is a single point in the unloaded condition. However, upon application of the load, the bearing surfaces deform elastically in the neighborhood of the point, causing the point to enlarge into a region.

CHAPTER II

APPLICATION OF THE THEORY TO AN EHD POINT CONTACT IN PURE SLIDING

The theory and rheological model of Jakobsen is applicable for finding the shear stress at a point in a sliding elastohydrodynamic contact. The theory may be applied to a determination of the traction force by evaluating the shear stress at a number of locations in the contact and integrating over the contact area. It is the aim of this chapter to summarize the theory and to illustrate its application to an EHD point contact.

Summary of the Theory

The assumptions which form the basis for the theory, presented in detail in Jakobsen 1973 (1) and Jakobsen and Winer 1974 (2), are restated here for convenience. The lubrication situation, with major assumptions, is as shown in Figure 1. Surface 1 is stationary, and surface 2 moves with constant velocity in the x_1 - direction, $u_1 = UH$. The film thickness is h.

According to both theory and experiments, the change of film thickness over most of an EHD contact is very small compared with the size of the contact. The bearing surfaces are therefore assumed parallel in the vicinity of the point

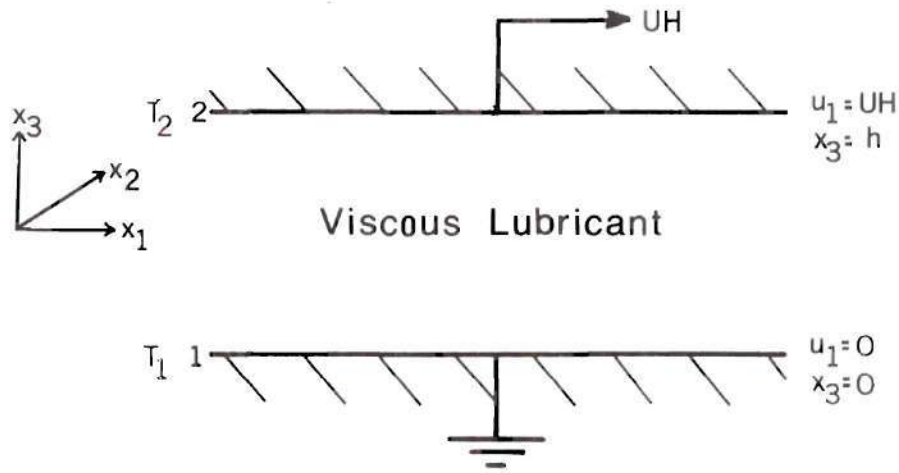

Assumptions

1. $u_1 = u_1(x_3)$; $u_1(0) = 0$; $u_1(h) = UH$
2. $u_2 = u_3 = 0$
3. p = constant
4. $T = T(x_3)$; $T(0) = T_1$; $T(h) = T_2$
5. ρ = constant
6. k = constant

Figure 1. The Lubrication Situation, with Major Assumptions.

at which the shear stress is being calculated, although film thicknesses are allowed to vary from point to point.

While temperature variations are recognized to exist in the x_1 - and x_2 - directions, the gradients of temperature in these directions are much smaller than in the x_3 - direction. Typical experimental data shows an average temperature gradient over the film thickness (i.e. in the x_3 - direction) of approximately 5×10^{8} ^{o}K/m (2×10^{7} ^{o}R/in); in the x_1 and x_2 - directions, an average gradient over the contact is 9×10^{4} ^{o}K/m (4×10^{3} ^{o}R/in). This represents a difference of four orders of magnitude. Therefore, temperature is assumed to be pointwise independent of x_1 and x_2. Furthermore, since the effect of convection is shown to be small compared with conduction in the x_3 - direction, the resulting distortion of flow velocities is neglected.

Because surface 2 is moving, the major portion of heat generated through viscous dissipation is carried away by this surface, and the stationary surface, 1, is assumed adiabatic. Over the major portion of the contact, the component of shear stress due to the pressure gradient is much smaller than that due to sliding motion. Consequently, the pressure is assumed pointwise constant. Detailed discussion of these last two assumptions is found in Jakobsen 1973 (1) Chapter V. In addition, body forces are neglected, and density and thermal conductivity are assumed constant.

A Newtonian rheological model of the lubricant, em-

ploying a linear relationship between shear stress and shear rate, is used. The viscosity is the coefficient of proportionality, and is a function of pressure and temperature. As mentioned previously, the viscosity-temperature dependence is expressed by the power-exponential function

$$\mu = \eta/c_1 = e^{(E/T)^Q} \tag{1}$$

where μ is the dimensionless viscosity, c_1 is a dimensioned constant (= 10^{-3} Ns/m^2 when η is in Ns/m^2), E is a characteristic temperature, and Q is a temperature-viscosity coefficient. Both E and Q are functions of pressure. Jakobsen 1973 (1) has shown that Equation (1) gives a reasonable description of lubricant viscosity within the range of temperature and shear stress normally found in an elastohydrodynamic contact.

Through integrations of the energy equation and the equations of motion, reduced by the above assumptions and the given rheological model, the theory provides a means of calculating the shear stress τ at any point in a sliding elastohydrodynamic contact. The following parameters must be known: the temperature of the moving surface, T_2; the film thickness, h; the thermal conductivity of the fluid, k, the sliding speed, UH; and the viscosity parameters, Q and E. These latter two are found by taking, from viscometric data on the

lubricant, the viscosity at two different temperatures and the pressure at the point in question, and solving equation (1) for Q and E. This calculation is represented in the form of dimensionless charts in the appendix to Jakobsen and Winer 1974 (2), and has also been incorporated into the computer program of the following chapter. It should be noted that E has units of temperature and that Q is dimensionless. In this work, the temperatures at which the viscosity is taken are 38° and 99° (100° and 210° F). These are two temperatures at which standard viscometric measurements are often made, and they also correspond roughly to the range of temperatures expected for an EHD contact operating under average conditions.

In order to select these viscosities from the lubricant data, the pressure at the point in question must be known. Therefore, some assumption about the pressure distribution in the contact has to be made. Jakobsen 1973 (1) suggests the use of a Hertzian distribution as an approximation to the actual pressures, which may in fact depend on lubricant properties and operating conditions. The computer-generated solutions to the EHD problem summarized in Dowson and Higginson 1966 (13) and those of Cheng and Sternlicht 1965 (8) show pressure distributions which appear to converge to the Hertzian as the speed decreases and the load increases. The major deviations from the Hertzian in these solutions occur in two areas. First, the solutions tend to exceed the

Hertzian pressures near the inlet, where pressures are lower than at the center and the film thickness is larger; therefore, this deviation is not expected to contribute significantly to the total traction. The computer solutions also show a sharp pressure spike on the outlet side; the width of the spike, however, seems to indicate that its integrated effect on the total traction will be small.

It should be emphasized that Jakobsen's theory does not require the use of a Hertzian pressure distribution. There is currently a great deal of controversy about the actual shape of the pressure distribution in EHD contacts, due in part to a shortage of reliable experimental data. However, in this traction study, the Hertzian distribution is used because of its simplicity and its apparent applicability to a wide range of operating conditions.

Application to Traction Calculations

In the present work, the basic equations of the theory summarized above are solved numerically through the use of a Fortran computer program. The program was designed to evaluate the shear stress at various points in the EHD contact, and to perform a numerical integration over the contact area to yield the traction force.

Using Jakobsen's 1973 (1) dimensionless notation, the condition of an adiabatic stationary wall is shown to result in the relation

$$\pi_4 = - \int_{\pi_1}^{\pi_2} \mu(\theta, \pi_3)^{-1} d\theta \tag{2}$$

where

$$\pi_1 = T_1/E \qquad \pi_2 = T_2/E \qquad \pi_3 = Q$$

$$\pi_4 = \frac{c_1 (UH)^2}{2k \quad E} \qquad \theta = T/E$$

and $\mu(\theta, \pi_3)$ is the assumed viscosity function, dependent on temperature and pressure. The only unknown in (2) is π_1, so that this equation may be used to solve for the temperature of the stationary wall at the point under consideration. This is accomplished by introducing the arbitrary temperature π_o ($\pi_o << \pi_2$) and rearranging (2) to yield

$$\int_{\pi_o}^{\pi_1} \mu(\theta, \pi_3)^{-1} d\theta = \int_{\pi_o}^{\pi_2} \mu(\theta, \pi_3)^{-1} d\theta + \pi_4 \tag{3}$$

The right hand side is evaluated on the computer by performing a numerical integration from π_o to π_2 and adding in the computed value of π_4. A similar integration is performed on the expression on the left side of (3), stopping when the value of the integral is equal to the right side of the equation. At this point, the temperature π_1 has been reached in the integration, and is therefore determined.

Once the stationary surface temperature is evaluated in this manner, the shear stress may be found from

$$\pi_5 = 1/2\ \pi_4^{-1/2} \int_{\pi_2}^{\pi_1} [\pi_4 - \int_{\pi_2}^{\theta} \mu(\xi,\pi_3)^{-1} d\xi]^{-1/2} d\theta \qquad (4)$$

where π_5 is the dimensionless shear stress given by

$$\pi_5 \equiv \frac{\tau h}{c_1 (UH)}$$

All parameters on the right-hand side of equation (4) are known, so that it may be evaluated numerically and the shear stress at the point determined.

This process of calculating the shear stress at a point is repeated systematically throughout the Hertzian contact. The stress is evaluated at equal intervals along the centerline of the contact, as well as along one or more lines parallel to the centerline (see Figure 2a). To facilitate the numerical integration method used, there must be an odd number of points in each of these lines. Symmetry of the flow geometry about the centerline is taken advantage of in evaluating the stress throughout the contact. It then remains to calculate the double integral of the shear stress over the contact area to determine the traction. That is,

$$Tr = \iint_{\text{contact}} \tau\ dx_1 dx_2 \qquad (5)$$

Integration is the x_1 - direction along each of the lines of shear stress is done numerically by Simpson's method.

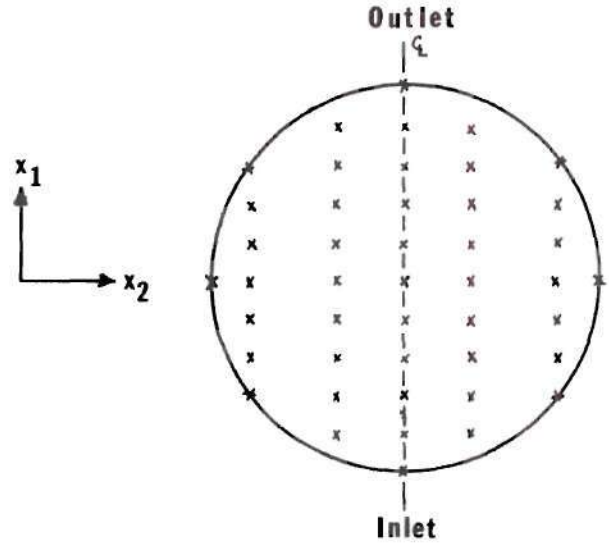

2a. Typical Contact Locations of Points for Shear Stress Calculation

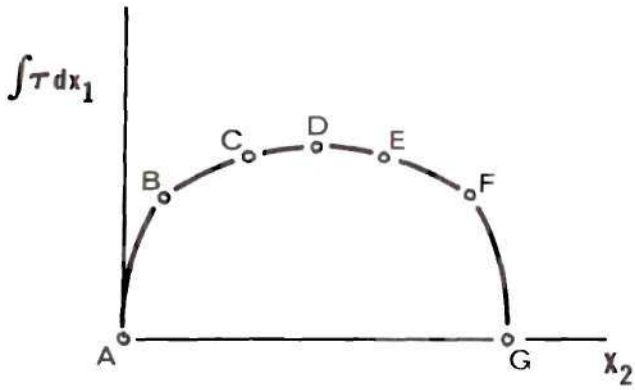

2b. Integration in the x_2 - direction

Figure 2. Traction Calculation by Numerical Integration.

This is made possible by the equal spacing and the even number of intervals between points in each of these lines.

Since it is not always convenient, however, to have the lines themselves spaced equidistant from one another, Simpson's method may not be used without modification for integration in the x_2 - direction. Simpson's composite rule is based on passing connected parabolic segments through equally spaced data points and calculating the sum of the areas under each of these segments as an approximation to the integral. This same general method may be applied to the case here where the spacing is irregular.

Referring now to Figure 2b, since the values of both the abscissa and the ordinate of points A, B, and C are known, a parabola may be passed through these three points by the use of Newton's divided difference formula (see Scheid 1968 (16)). This parabola is then integrated using the abscissas of points A and C as limits of integration. The process is repeated using, in turn, points C, D, E, and points E, F, G. The only requirement is that, since three points are used at a time, there must be an even number of intervals across the contact. This is automatically satisfied by the symmetry about the centerline - for every interval to the left of center, there is a duplicate interval to the right. Truncation error using this method is expected to be comparable to that of Simpson's method, since both use a quadratic approximation.

In this way, the shear stress is calculated and integrated over the surface of the contact to determine the traction force. The Fortran program written to perform these calculations is listed and documented in Appendix B.

CHAPTER III

COMPARISON OF MEASURED AND CALCULATED TRACTIONS

Experimental measurements of the traction is an elastohydrodynamic point contact in pure sliding were made, and the results compared to calculations using the theory summarized in Chapter II. The contact consisted of a rotating steel ball whose surface slid with constant speed on a stationary flat surface of synthetic sapphire. Dimensions and physical parameters of the contact are given in Appendix A. Both measurements and calculations were made at sliding speeds ranging from .35 to 12.7 meters per second (13.7 to 500 inches per second), and at normal loads of 67 and 334 newtons (15 and 75 pounds). The lubricant used was a naphthenic hydrocarbon oil, designated as Fluid N1 in Sanborn 1969 (17) and Sanborn and Winer 1973 (18,19), and as Fluid F in Novak 1968 (20). Physical characteristics of the fluid may be found in these references.

Traction Calculations

Initial calculations were made based on a normal load of 67 N (15 lb.), and sliding speeds of .35, .70, 1.40, 2.54, 5.1 and 12.7 m/s (13.7, 27.4, 55, 100, 200, and 500 ips). The load resulted in a peak Hertzian pressure of approximately

1.03×10^9 N/m^2 (150,000 psi) and a circular contact with a Hertzian radius of .18 mm (.007 in).

The temperature distribution on the surface of the moving ball for each of the sliding speeds was known from measurements made using the infrared technique described in Turchina, Sanborn, and Winer 1973 (7). The distribution of film thickness in the contact area was also known from measurements made using the optical interference technique of Sanborn 1968 (7) and Sanborn and Winer 1973 (18).

The required pressure-viscosity data for the fluid N1 was obtained from Novak 1968 (20). However, because the viscosity data was only recorded at pressures up to 1.38×10^8 N/m^2 (20,000 psi.) at both 38° and 99°C (100° and 210°F), it was necessary to extrapolate the experimental curves up to the maximum Hertzian pressure of 1.03×10^9 N/m^2 (150,000 psi). This extrapolation was performed using Roelands' 1966 (21) pressure-viscosity correlation, given by the equation:

$$\log \eta - 1.8 = (\log \eta_o - 1.8)(1 + \frac{p}{1.96 \times 10^8})^Z \qquad (6)$$

where η_o is the viscosity at atmospheric pressure, Z is a parameter which is independent of pressure, η and η_o are in Ns/m^2 and p has units of N/m^2.

Calculation of the shear stresses along the centerline and along only one additional parallel line .13 mm (.005 in) from the centerline was found to yield sufficient accuracy.

The points at which these calculations were made were separated by a distance of .025 mm (.001 in) in each line. Pressures at each point were computed from the Hertz equation for a point contact

$$p = \frac{p_{hz}}{a}(a^2 - r^2)^{1/2} \tag{7}$$

where a is the radius of the contact and r is the distance of the point from the center of the contact. Viscosities at these pressures were then found from the correlation of equation (6).

At this point, all necessary input data for the determination of the traction at the six speeds was known, and the program could be run. The results are given in the form of traction coefficients, defined as the ratio between the traction force and the normal load. Computer output from a typical run is shown in Appendix C.

Ball temperature and film thickness data were also available for conditions of a 334 N (75 lb) normal load and speeds of .70, 1.40, 2.50, and 5.1 m/s (27.4, 55, 100, and 200 ips). The resulting Hertzian contact had a radius of .30 mm (.012 in) and maximum Hertzian pressure was approximately 1.7×10^9 N/m^2 (250,000 psi). The shear stress was again calculated at points separated by .025 mm (.001 in) along two lines - the centerline and a parallel line .203 mm (.008 in) from the centerline. Pressure calculations and

viscosity extrapolations were made as in the case of the 67 N (15 lb) load.

Results of the traction calculations are summarized in Table 1.

Table 1. Calculated Traction Coefficients

Sliding Speed m/s (ips)	Traction Coefficient 67 N (15 lb) Load	334 N (75 lb) Load
.35 (13.7)	.432	--
.70 (27.4)	.212	.199
1.40 (55)	.084	.078
2.50 (100)	.042	.045
5.1 (200)	.028	--
12.7 (500)	.012	--

Traction Measurements

The traction force for each of the conditions of load and speed of the previous section was measured using the experimental apparatus described in detail in Sanborn 1969 (17) and Sanborn and Winer 1973 (14). In this set-up, the normal load is applied to the rotating steel sphere. The sphere, support, and loading mechanism are mounted on an air bearing which provides rigidity in the vertical direction and friction-free movement in the direction parallel to the sliding velocity. During operation, the traction force causes the bearing assembly to be displaced in this direction.

This force is measured by means of a load cell consisting of strain gages mounted on a cantilever beam.

For the case of the 67 N (15 lb) load, it was not possible to obtain a traction reading at a speed of 12.7 m/s (500 ips), due to excessive vibrations in the system at this speed. Measurements were obtained at the other five sliding speeds, however.

When the load was increased to 334 N (75 lb), it was necessary to increase the stiffness of the traction load cell and recalibrate, in order to prevent excessive deflections due to the higher traction force expected. In addition, sufficient pressure could not be developed in the air bearing to support the higher normal load. Consequently, oil was used in the bearing in place of air. This, of course, increased the viscous friction in the bearing, but, due to the presence of a full oil film, coulomb friction remained absent and the traction reading was essentially unaffected.

Results of the traction measurements are shown in Table 2 for both loading conditions.

Table 2. Measured Traction Coefficients

Sliding Speed m/s (ips)	Traction Coefficient 67 N (15 lb) Load	334 N (75 lb) Load
.35 (13.7)	.156	--
.70 (27.4)	.128	.046
1.40 (55)	.074	.045
2.54 (100)	.059	.041
5.1 (200)	.042	--

Comparison of Results

Figure 3 shows a plot of both calculated and measured traction coefficients against sliding speed for the 67 N (15 lb) load. Figure 4 is a similar plot for the 334 N (75 lb) load.

Both figures indicate that the calculated and measured curves begin to diverge rather strongly as speed decreases below a certain point. For the 67 N (15 lb) load, this point occurs at about 1.5 m/s (60 ips) while it is somewhat greater than 2.5 m/s (100 ips) for the 334 N (75 lb) load.

Because the film thickness decreases as the sliding speed decreases, there is a possibility that this divergence is related to asperity interaction. Such interaction may affect the traction in two ways. First, contact between asperities on the ball and on the sapphire would tend to resist the sliding motion, thus increasing the measured traction. Second, such interaction would generate heat which would in turn lower the viscosity of the lubricant in the film, causing the traction to decrease. The traction model used for the calculations assumes that the only source of heat in the EHD contact is that due to viscous shearing of the lubricant. Therefore, if the second mode of asperity interaction is the dominant one in the cases under consideration, one would expect the calculated tractions to exceed the measured values, this did in fact occur at low speeds. The computational model

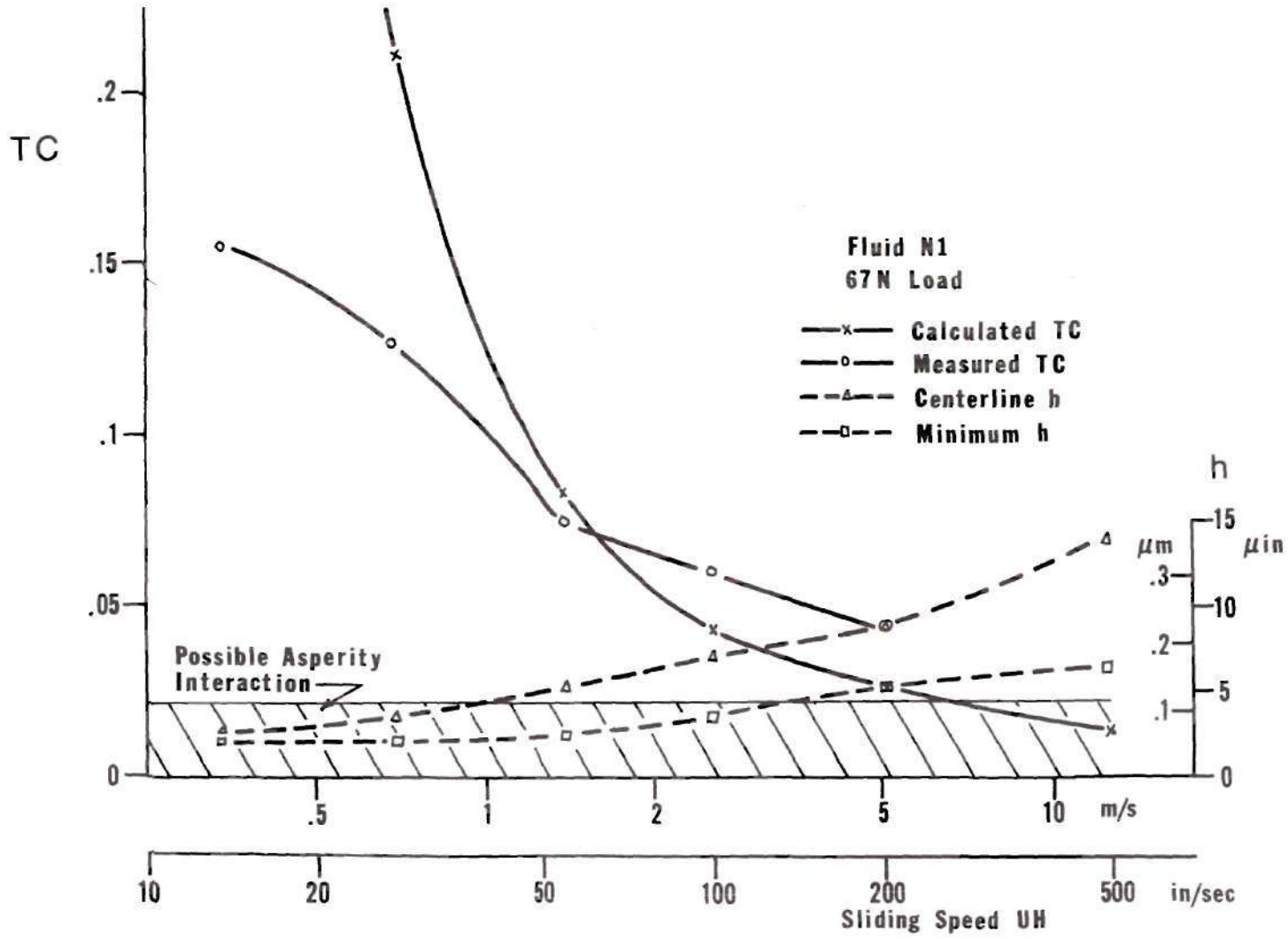

Figure 3. Calculated and Measured Traction - Low Load.

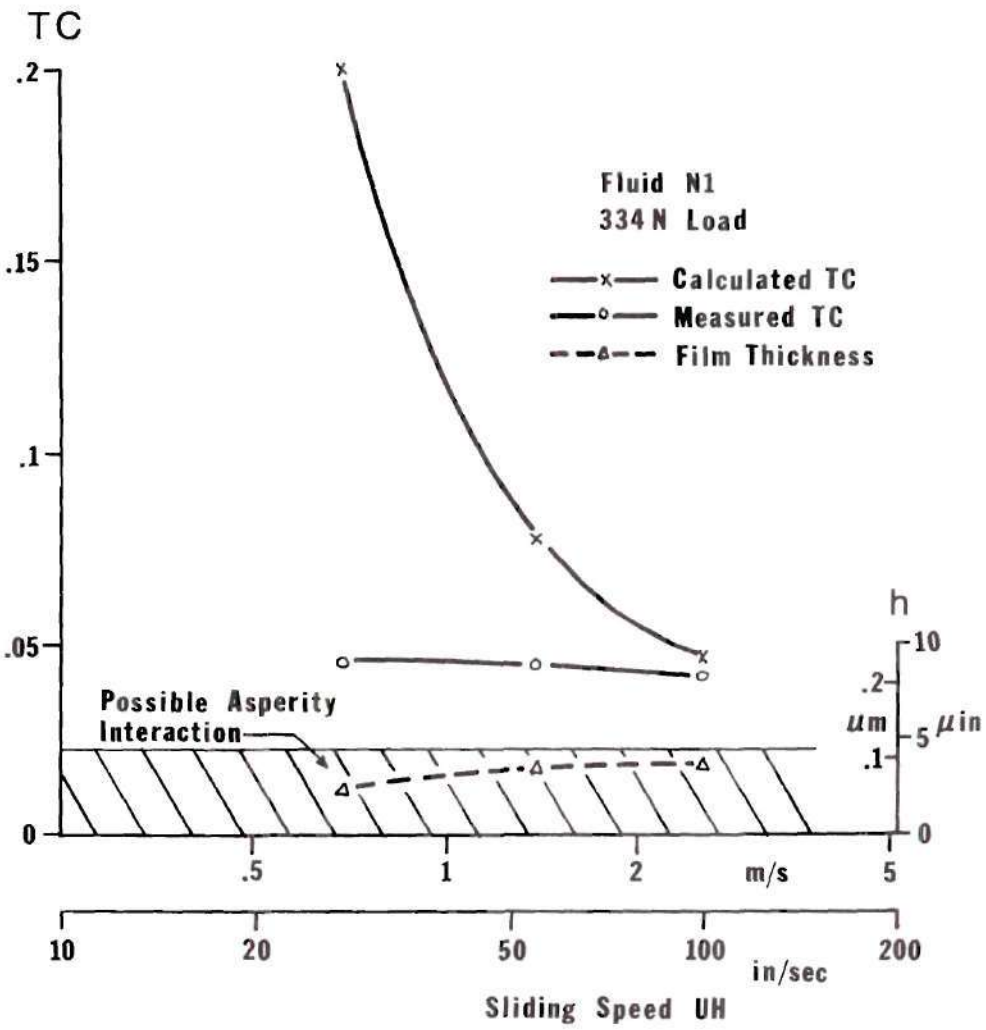

Figure 4. Calculated and Measured Traction - High Load.

ignores the heat generated by the asperity contact; consequently, calculated film temperatures are less than actual ones, so that fluid viscosity is higher, resulting in a higher calculated traction.

In addition, as the film thickness decreases, it is possible that the asperities themselves carry a part of the load, thus decreasing the pressure on the fluid. This would result in lower viscosity and therefore a lower traction than in the case of a full fluid film. Figures 3 and 4 show that calculated tractions do exceed measured values at low speeds.

In order to further investigate the possibility of asperity interactions, surface profiles of both the steel ball and the sapphire were recorded on a Bendix Group XV Proficorder. The rms peak-to-valley surface roughness was found to be approximately .033 μm (1.3 μin.) for the ball and .013 μm (0.5 μin.) for the sapphire, yielding a composite peak-to-valley roughness of .046 μm (1.8 μin.). In addition, the centerline and minimum film thickness measurements were recorded as a function of speed in Figures 3 and 4 (for the high load, the centerline and minimum film thicknesses were the same). From Figure 3, the centerline film thickness where the two traction curves cross was about .13 μm (5 μin.), and the minimum film thickness was .064 μm (2.5 μin.) there. In the case of the high load, the film thickness at the point of crossing was approximately .089 μm (3.5 μin.). It is

interesting to note that this thickness for the high load case, in which the surfaces are nearly parallel over the entire contact, was bracketed by the minimum and centerline values in the low load case, in which definite side lobes of minimum film thickness exist. Since this minimum occurs over a relatively localized area, the thermal effects of asperity interaction would not become important at the same minimum film thickness as in the case of the high load, where the minimum occurs over virtually the entire contact. Using this reasoning, the differing values of minimum film thickness, at which measured and calculated traction curves for the two loads cross, do not appear to be contradictory.

Since rms surface roughness is a statistical quantity, there are peaks in excess of the composite value of .046 μm (1.8 μin.). Therefore, the incipient of asperity interaction may be expected to occur when the ratio of composite surface roughness to film thickness (λ) is somewhat greater than 1.0. Sibley 1971 (23) predicts noticeable surface distress for $\lambda < 1.5$, and indicates some asperity interaction for λ up to 3.0. Accordingly, Figures 3 and 4 show the composite surface roughness along with the film thickness, and a band inside which films may be expected to experience some asperity interaction.

Using an average film thickness of .089 μm (3.5 μin.) for the two cases, λ is slightly less than 2.0 at the point where the traction curves begin to diverge. These figures

indicate that asperity interaction is a possibility in explaining the deviation of the traction curves of Figures 3 and 4, although it has not been proven to be the sole contributing factor.

Another consideration in explaining the disparity between calculated and measured results is the behavior of the fluid under the extreme conditions imposed by a low sliding speed. It may be unreasonable to assume that a single rheological model is adequate to describe lubricant behavior throughout such a wide range of operating conditions. Johnson and Roberts 1972 (24) suggest that, above some critical shear stress, the fluid film behaves in the manner of a plastic solid rather than a viscous liquid. The possibility therefore exists that the rheological model used in this work breaks down when the shear stress in the film reaches a limiting value.

For the 67 N (15 lb) load, the maximum shear stress calculated at 1.40 m/s (55 ips) was in the neighborhood of 8.0×10^7 N/m^2 (11,600 psi). Similarly, for the 334 N (75 lb) load at 2.54 m/s (100 ips) maximum shear in the contact was calculated to be 8.1×10^7 N/m^2 (11,800 psi). Each of these two cases corresponds to a point at which calculated and measured tractions began to deviate as the speed decreased. At higher speeds, calculated shear stresses were all lower than these values. At speeds lower than the transition speeds, these shear stresses were exceeded. The fact that

these maximum shear stresses were essentially the same lends credence to the possibility that the Newtonian rheological model of the lubricant used in the calculations fails to adequately describe fluid behavior at extremely high shear stresses. The maximum shear stresses at the transition speeds were close in magnitude to the critical shear stresses observed by Johnson and Roberts.

At higher speeds, and therefore larger film thickness and low shear stresses, agreement between calculations and measurements appears to be quite good. The two traction curves of Figure 3 compare favorably with respect to the variation of traction with speed. Furthermore, if the curves of Figure 4 may be extended to higher speeds, the comparison is again quite favorable. For the low load, the calculated values were lower than measured at high speeds; this appears also to be the case upon extension of the curves for the high load. Part of this difference in the magnitude of the results may be explained by the uncertainty in extrapolating the fluid viscosities to higher pressures, as discussed in the following section. Furthermore, it should be recalled that the traction was calculated only in the Hertzian contact area. It is possible that, under certain conditions, significant traction may be developed outside the Hertzian contact, particularly in the inlet region, and in cases where the assumption of a Hertzian pressure distribution may not be a good one.

In summary, the theory and rheological model under consideration yield reasonable results for the traction at sufficiently high sliding speeds. The calculated results differ significantly from measurements at low speeds, possibly due either to asperity interaction at low film thicknesses, or a breakdown of the rheological model at extremely high shear stresses.

The Effect of Material Parameters on Traction Calculations

Because of the extent of the extrapolation required to determine the fluid viscosity at the high pressures of the contact, different pressure-viscosity extrapolations were used to determine their effect on the calculated traction. In one approach, the shape of the pressure-viscosity curve for fluid N1 was taken to be the same as that for a similar naphthenic fluid (fluid 36-G of the ASME Pressure-Viscosity Report 1953 (22)). Data for this fluid was available up to 6.9×10^8 N/m^2 (100,000 psi) at 99 C (210 F) and 3.48×10^8 N/m^2 (50,000 psi) at 38 C (100 F). Traction results for this extrapolation were about 15% lower than those in Table 1. The viscosity extrapolated for the inlet temperature and the pressure at the center of the contact was less than that given by equation (6) by a factor of 3.

In a second case, a Roelands extrapolation was used, but it was based on the assumption of a 10% uncertainty in Novak's 1968 (20) viscosity measurements at 1.4×10^8 N/m^2

(20,000 psi). This resulted in changes of the viscosity at the center of the contact by a factor of up to 2.5, and deviations of approximately 10% from the tractions of Table 1.

Despite the differences in the tractions computed using the several viscosity extrapolations, the dependence of traction on sliding speed remained unchanged in all cases studied. The ratio between tractions at two given speeds remained constant, regardless of the method of viscosity extrapolation.

Results of this study of the effects of using various pressure-viscosity relations indicate that the traction model is fairly insensitive to changes in the pressure-viscosity dependence of the lubricant. The need for a great deal of extrapolation in the traction calculation may be regarded not so much as a weakness of the model, but rather as the result of a lack of data concerning the viscosity of this particular fluid at high pressures.

In order to examine the effect of temperature-viscosity dependence on the calculated traction, a fictitious fluid was used in the program. This fluid was assumed to have the same pressure dependence and the same viscosity at the inlet temperature of 38° C (100° F) as the naphthenic Fluid N1. Its viscosity at 99° C (210° F) was assumed to be greater than that of Fluid N1 by a factor of 2.8. This had the effect of reducing by 1/2 the exponential temperature-viscosity coefficient $\left|\frac{1}{\eta}\frac{d\eta}{dT}\right|$. The viscosity-temperature behavior of this

fictitious fluid is similar to that of a dimethyl siloxane, a lubricant with low temperature-viscosity dependence.

In this calculation, all other parameters in the EHD contact (e.g. film thickness, moving surface temperature, thermal conductivity) were assumed to be the same as those for Fluid N1 for identical load and speed. If such a fluid were used in the contact, the film thickness should in fact change very little, since it is at most weakly dependent on the temperature-viscosity coefficient. The surface temperature would probably be affected, however; keeping it the same as that for fluid N1 served only to isolate the effect of variations in the temperature-viscosity dependence of the fluid.

Calculations using this fluid resulted in a traction coefficient three times greater than that of Fluid N1 for the same conditions of load and speed. This indicates that the traction is increased by a decrease in the temperature-viscosity coefficient of the lubricant. The traction appears to be relatively sensitive to variations in the temperature-viscosity coefficient.

The effect of the base viscosity on the traction was also studied. Another fictitious fluid was used, having the same pressure dependence and the same temperature-viscosity coefficient over the range 38° - 99° C (100° - 210° F) as Fluid N1, but having a viscosity at 38° C (100° F) three times that of Fluid N1. Again, all other system parameters were

held constant. The resulting traction coefficient was greater than that for Fluid N1 by a factor of 1.75. The traction therefore increases as the inlet viscosity increases.

The only other lubricant parameter which is involved in the traction calculation is the thermal conductivity. In a study of Jakobsen's theory, Lambelet 1973 (25) shows a slight increase in the shear stress as the thermal conductivity of the fluid increases. Furthermore, Carlson, et. al. 1973 (26) indicate that the thermal conductivities for most hydrocarbon and methyl siloxane lubricants fall within a 10% range. Therefore, the thermal conductivity is not a strong factor in determining the traction.

The above study indicates that the primary lubricant property variations which cause an increase in the traction are an increase in the inlet viscosity and a decrease in the temperature-viscosity dependence. Increasing the pressure-viscosity dependence also increases the traction, but apparently to a lesser extent. Variations in thermal conductivity appear to be of minor importance.

In the actual substitution of fluids with different material parameters, traction variations of the magnitude indicated above are not to be expected. This is primarily because the surface temperatures for Fluid N1 were used in the calculations. Using a more viscous fluid, for instance, would increase the energy dissipation in the contact, thus increasing the temperature, and therefore decreasing the

traction until a lower steady state value is reached with higher surface temperatures. Temperatures and film thicknesses for Fluid N1 were used only so as to allow independent variation of the material parameters. Consequently, the results of the calculations of this section should be viewed as relative variations only, rather than absolute magnitudes to be expected in actual lubrication situations.

CHAPTER IV

CALCULATION OF FILM THICKNESS

In order to apply Jakobsen's theory to determining the traction in an elastohydrodynamic contact, the film thickness must be known throughout the contact. In the previous chapter, film thickness measurements were used for the purpose of evaluating the theory. However, in most engineering applications, such measurements will not be available. It is therefore desirable to have some means of calculating the film thickness.

Because thermal effects are less important in film thickness analyses than in traction studies, most film thickness formulas are based on isothermal conditions. In addition, a large number of such formulas are expressed in terms of the dimensionless groups discussed in Dowson and Higginson 1966 (13). Cheng 1972 (27) lists several of these formulas, most of which apply only to line contacts. The formula of Archard, however, is applicable to point contacts, and therefore is the one which was studied. It is expressed as

$$h/R = 1.37\ G^{.74}\ U^{.74}\ P_{hz}^{-.22} \qquad (8)$$

where the dimensionless groups are

$$G = \alpha E' \qquad U = \frac{\eta_o (U_1 + U_2}{2\ E'\ R} \qquad P_{hz} = \frac{p_{hz}}{E'} \tag{9}$$

In equations (9), p_{hz} is the peak Hertzian pressure, E' is the reduced elastic modulus of the system, R is the reduced roller radius (equal to the ball radius in our system), and $(u_1 + u_2)$ = UH in the notation of this work. η_o and α come from the exponential pressure-viscosity relation

$$\eta = \eta_o\ e^{\alpha p} \tag{10}$$

Equation (8) yields a value for the nominal film thickness. Although the film thickness may vary slightly throughout an actual EHD contact, the surfaces are nearly parallel, so that a single calculated value, such as that given by equation (8), may be used as a first approximation for the purpose of traction calculations. The effect on the shear stress calculation of using a single film thickness throughout the contact in a typical case is shown in Figure 5. The figure shows that, if the constant film thickness chosen is representative of the actual contact, the shear stress integrated over the contact would be affected only slightly.

Before using a film thickness calculation in place of experimental data, it is useful to know the effect which inaccuracies in the result will have on the calculated traction. From the definition of the parameter π_5, it is seen that

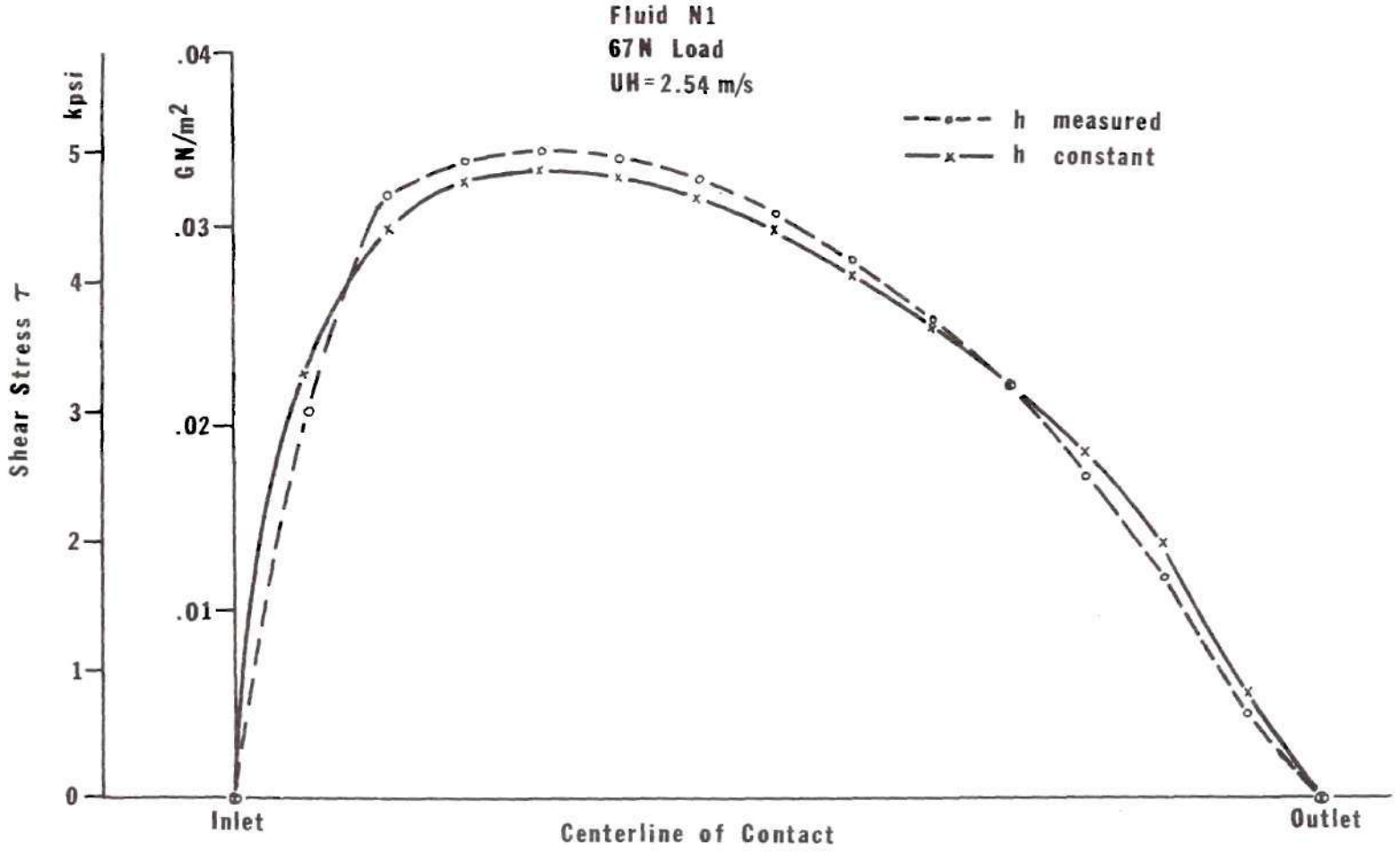

Figure 5. Typical Centerline Shear Stress Distribution.

$$\tau = \frac{c_1 (UH) \pi_5}{h}$$

That is, the shear stress at a point is inversely proportional to the film thickness. This strong dependence of the traction on film thickness indicates that the traction calculation is only as good as the film thickness used. An accurate calculation of the film thickness is therefore essential to the success of the traction determination.

Appendix D lists the results of film thickness calculations compared to measurements for a number of fluids at various speeds, along with a description of the fluids. Based on these comparisons, several conclusions may be drawn as to the use of equation (8) in predicting the film thickness.

Many lubricants do not strictly exhibit the exponential pressure-viscosity behavior of equation (10); that is, α may be a function of pressure. Therefore, following the suggestion of Jakobsen, Sanborn, and Winer 1974 (28), α^* was used in equation (8) when available. α^* is found by integrating the experimental viscosity data over the entire pressure range.

$$\alpha^* = [\eta_o \int_o^\infty \frac{dp}{\eta(p)}]^{-1} \tag{11}$$

This makes α^* less dependent on any single viscosity data

point, and accounts for the variation of α with pressure. It may therefore be thought of as a representative value of α over the range of pressures in the contact.

Both η_o and α^* vary with temperature. Consequently, the temperature at which they are evaluated affects the calculated film thickness. In most cases, the inlet temperature yields satisfactory results. For the calculations summarized in Appendix 4, data for α^* and η_o was available at 100° F, which roughly corresponds to the inlet temperature at which the measurements had been made.

As the sliding speed increases, the isothermal assumption used in developing equation (8) becomes less applicable. Shear heating of the lubricant at the inlet as it is forced between the bearing surfaces tends to decrease its viscosity and therefore decrease the film thickness. Greenwood and Kauzlarich 1973 (29) developed a formula for the computation of a thermal reduction factor ϕ_T, the factor by which film thickness is reduced due to inlet heating. ϕ_T was calculated for several of the cases listed in Appendix D in order to evaluate heating effects in these instances. In all cases, ϕ_T was greater than .90, and exceeded .95 in the large majority of calculations. Due to its relatively small effect, the thermal reduction factor was not incorporated into the calculations of this study. In some cases of very high speed operation, however, its use may be warranted.

From Figures 8-11 of Appendix D comparing calculated

and measured film thicknesses, several conclusions may be drawn as to the applicability of Archard's film thickness formula to various types of fluids. Results of calculations using siloxane fluids were not particularly favorable (Figure 8). This is most probably due to the tendency of these fluids to exhibit non-Newtonian behavior at elevated shear stress (see Jakobsen, Sanborn, and Winer 1973 (28)). In contrast, calculated results for the ordinary mineral oils correlate relatively well with measurements (Figures 9-11). Figures 9 and 10 indicate, however, that for polymer-blended hydrocarbon oils, the viscosity parameters of the base oil alone should be used. This is possibly a result of molecular degradation of the polymers in the EHD contact (see Walker, Sanborn, and Winer 1974 (30)).

The capability to calculate film thickness using Archard's formula has been incorporated into the computer program listed in Appendix B. It was designed such that, by changing the input data, the same program may be used regardless of whether the film thicknesses are calculated or read in as input.

CHAPTER V

CALCULATION OF MOVING SURFACE TEMPERATURE

As in the case of film thickness, it is not always possible to measure the temperature of the moving surface for the purpose of calculating tractions. It is desirable to have available a means of calculating the temperature distribution on the surface.

The contact may be thought of as a circular source of heat energy moving with constant speed across the surface of the ball. Although the temperature distribution due to a moving circular source has not been analytically treated in detail, the problem of an infinitely wide band source of constant magnitude has been solved, and the results presented in Carslaw and Jaeger 1959 (31). Furthermore, Jaeger 1942 (32), in his original paper on the subject, shows that the temperature distribution due to the band source is similar in magnitude and shape to that of a square source, particularly at high speeds. This implies that the width of the source is not important, so that the temperature due to the circular source may be approximated by that of the band source. This is particularly convenient since the results of the latter analysis may be approximately expressed by a simple algebraic formula. The temperature rise at a point is given by

$$\Delta T_2 = \frac{2q}{k_{tb}}\left(\frac{\kappa}{\pi(UH)}\right)^{1/2} x^{1/2} \tag{12}$$

when the source is located over the point, and by

$$\Delta T_2 = \frac{2q}{k_{tb}}\left(\frac{\kappa}{\pi(UH)}\right)^{1/2}[x^{1/2} - (x-\ell)^{1/2}] \tag{13}$$

after the source has passed the point. In equations (12) and (13), q is the strength of the source (heat per unit time per unit area), k_{tb} and κ are the thermal conductivity and thermal diffusivity, respectively, of the ball, x is the distance of the point from the leading edge of the source, and ℓ is the length of the source in the direction of motion.

It is worthwhile here to examine the conditions and assumptions made by Jaeger in deriving equations (12) and (13), and to compare them to the physical situation in the EHD contact. Both the velocity and the strength of the heat source must be constant. The sliding body (in this case the film) must be a non-conductor so that all of the heat generated is taken up by the surface.

This last assumption deserves closer examination. Allowing the moving substance to be a heat conductor complicates the results considerably. If this is the case, a fraction of the heat generated over the contact area passes to the moving surface, rather than the entire quantity of heat being taken up by the stationary surface. According to

Jaeger, this fraction, which may be calculated, depends on the thermal properties of the two materials and on the sliding speed. For the EHD contact considered here, the fraction of heat which goes into the film was calculated to be considerably less than 1%. In addition, Jakobsen 1974 (1) has asserted that heat conduction parallel to the surfaces is relatively unimportant in the EHD contact, so that the assumption of a uni-directional heat flux implicit in equations (12) and (13) is expected to be valid.

The assumption of constant speed is obviously satisfied, which leaves only the assumption of a constant heat source. The strength of the heat source at any point in the contact is the energy liberated per unit area per unit time, which is given simply by

$$q = \tau(UH) \tag{14}$$

(see Cameron 1966 (33)). Since the shear stress varies over the contact area, q is not a constant. Substitution of equation (14) into (12) and (13) yields, respectively,

$$\Delta T_2 = \frac{2\tau}{k_{tb}}\left(\frac{\kappa(UH)}{\pi}\right)^{1/2} x^{1/2} \tag{15}$$

$$\Delta T_2 = \frac{2\tau}{k_{tb}}\left(\frac{\kappa(UH)}{\pi}\right)^{1/2} [x^{1/2} - (x-\ell)^{1/2}] \tag{16}$$

In each of these equations, the temperature rise is a linear function of the shear stress. Therefore, the method of superposition applies, and the variable shear stress distribution along any line parallel to the direction of motion may be approximated by a series of shear stress segments of constant magnitude along their length. The total temperature rise at a point is then the sum of the contributions from each of these segments. For illustrative purposes, a set of shear stress segments to approximate a typical centerline traction distribution is shown in Figure 6.

This approach to determining the temperature of the moving surface may then be applied to each of the lines in the contact along which the traction is to be determined. Since the temperature calculation requires a known shear stress distribution, and the shear stress computation requires a known temperature distribution, an iteration procedure was set up which proceeds as follows:

(1) Assume a shear stress distribution along the line of the contact.

(2) Use this assumed distribution to calculate moving surface temperatures.

(3) Calculate the shear stress distribution based on the temperatures of step (2).

(4) Compare assumed and calculated shear stress distributions. If the convergence criterion is satisfied, terminate. Otherwise, revise the assumed distribution and return

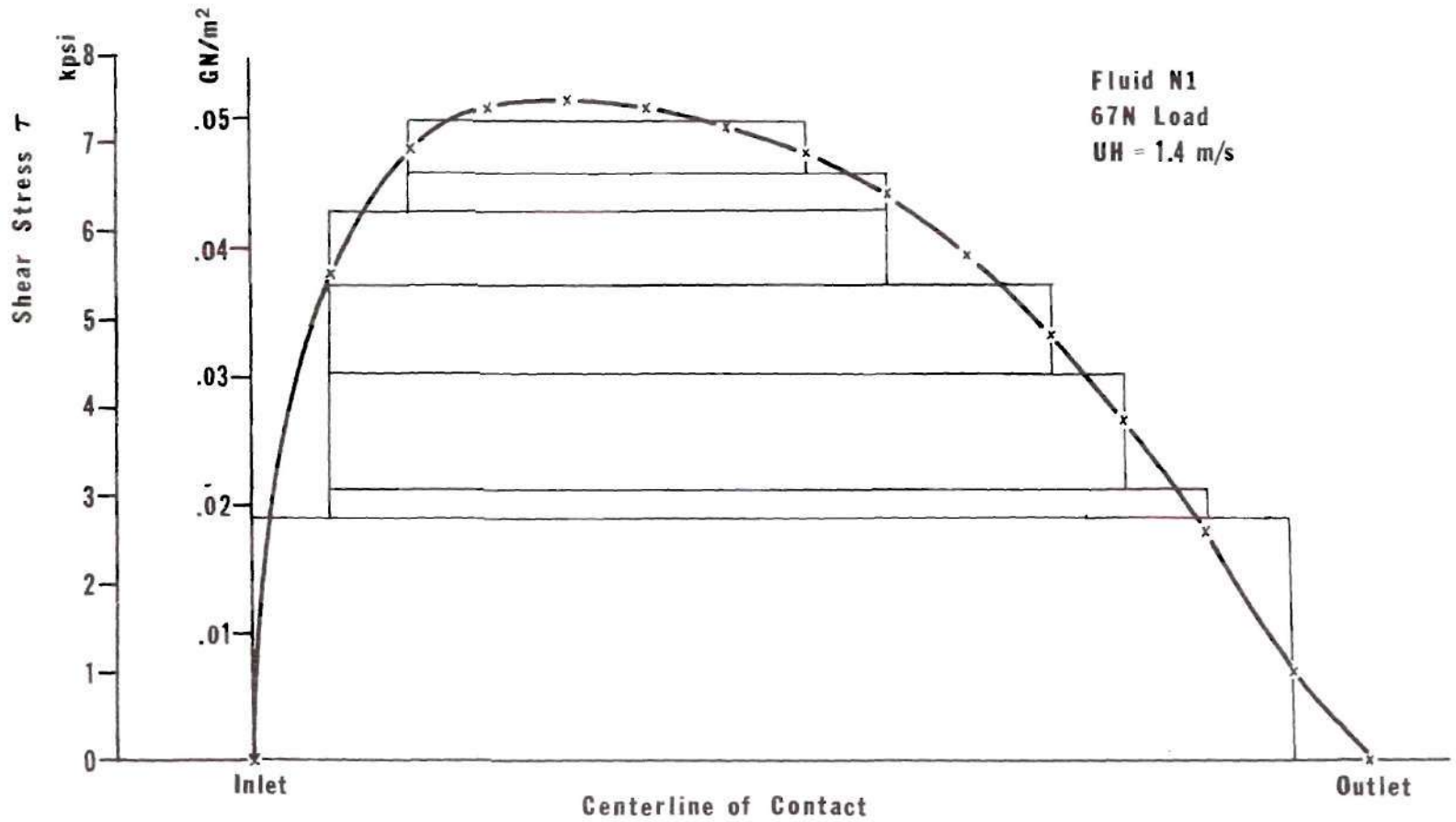

Figure 6. The Set-up of Shear Stress Segments along the Centerline.

to step (2).

Using this method, the only required temperature data is the inlet temperature of the moving surface. This may be estimated, since calculations have shown that the final distributions are not very dependent on this inlet temperature.

The procedure for setting up a segmented shear stress distribution from the assumed distribution, calculating the temperatures at the moving surface, and performing the iteration process outlined above were incorporated into the computer program in Appendix B. Therefore, as in the case with the film thickness, the program has the capability to calculate the traction whether or not detailed moving surface temperature data is available.

Convergence of the iteration scheme is said to occur either when the average calculated shear stress along the line changes by less than 0.2% in successive iterations, or when the difference between the assumed and average shear stress at each point on the line is less than 5%. The program incorporates an ad hoc method of updating the assumed shear stress distribution which was found, by several trials, to speed the convergence process. Convergence along each line is generally achieved in seven or fewer iterations; if convergence has not been attained after 10 iterations, the process is terminated and the results up to that point printed out.

An evaluation of the validity of this application of

Jaeger's temperature formulation to the EHD contact, independent of Jakobsen's traction model, was attempted. Using the experimental ball temperatures employed in the calculations of Chapter III, the inverse process of that described above was performed. That is, equations (15) and (16) were used to find the distribution of shear stress over the contact which would result in the measured temperatures. These shear stresses were then integrated over the Hertzian contact area to yield the tractions which, in turn, may be compared to the experimentally-determined tractions. These computations were performed for the five speeds and 1.03×10^9 N/m^2 (150,000 psi) peak Hertz pressure. The results are shown in Figure 7.

The traction coefficients predicted by the temperature model alone are seen to be significantly lower than those measured at low sliding speeds. This model depends only on the magnitude of the shear stress in the contact, regardless of any particular rheological model or the presence or absence of asperity interaction. Therefore, the disparity between the predicted and measured tractions of Figure 7 may not be explained by non-Newtonian lubricant behavior or by asperity interactions. However, as mentioned previously, the assumption that the moving circular source of heat may be approximated by a band source was shown by Jaeger 1942 (32) to be less valid at low speeds, and in the direction of the disparity in Figure 7. This is due to the greater role of

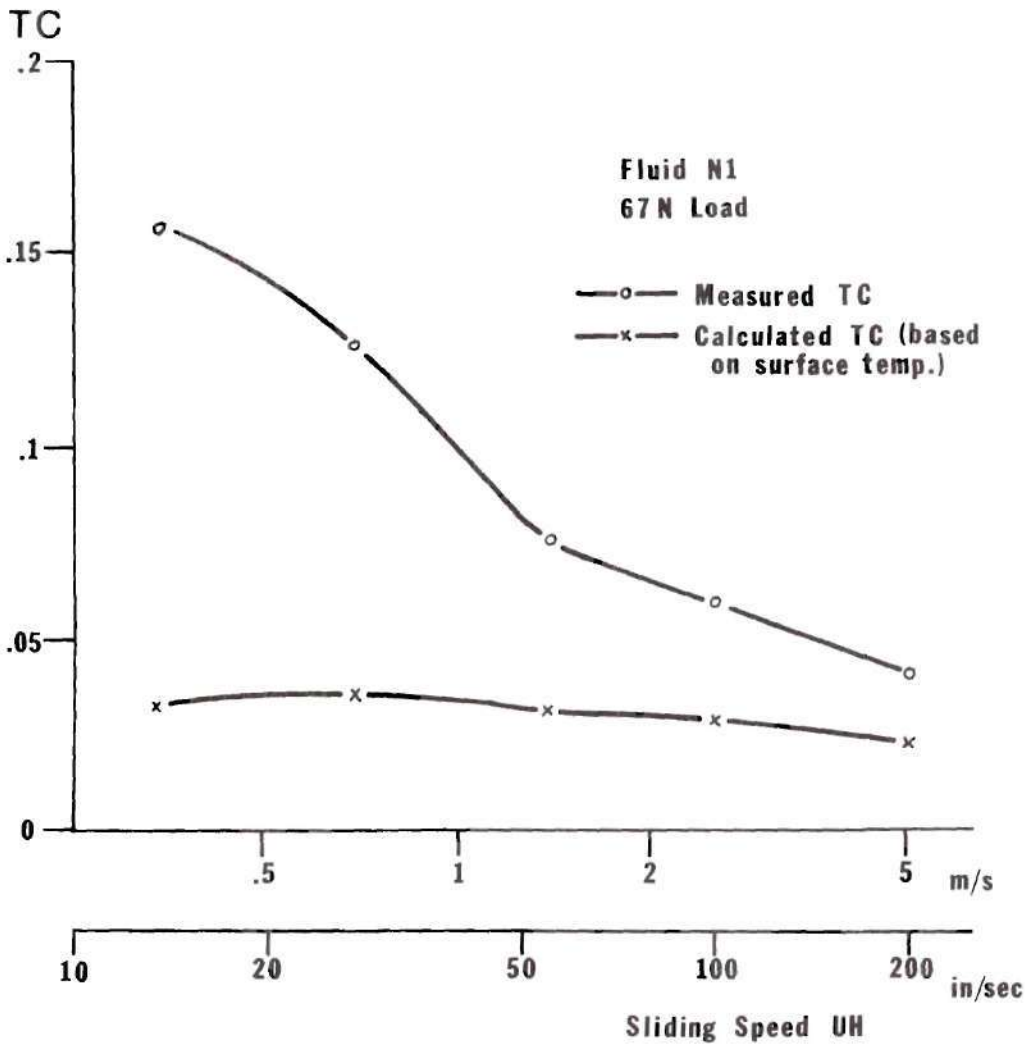

Figure 7. Traction Calculated from Measured Temperatures, Compared with Measured Traction.

end effects at lower speeds. The validity of the assumption depends on the magnitude of the dimensionless speed parameter

$$V = \frac{(UH)\ell}{2\ \kappa} \tag{17}$$

The parameter ℓ is the length of the shear stress segment, which is equal to or less than the diameter of the contact. As seen in Figure 6, the segment length becomes smaller near the top of the stack. Jaeger shows very good agreement between the band source and the source of finite width for $V \geq 10$. The value of V, for a speed of .70 m/s (27.4 ips) and shear stress segments of average length .20 mm (.008 in.), is 7.3. Therefore, for the lower speeds, and particularly for the calculations away from the centerline where shear stress segments are necessarily shorter, the model predicts significantly lower temperatures than measured.

In addition, the calculations on which Figure 7 is based evaluated the shear stress only within the Hertzian contact area. As mentioned in Chapter III, significant tractions may occur outside this area under certain conditions, which would also account for some of the discrepancy between the curves.

Although the above temperature model has been shown to be somewhat limited in its applicability, it should be noted that, in Jakobsen's theory, the dependence of the shear stress on the moving surface temperature is not particularly

strong. Lambelet 1973 (25), in a study of Jakobsen's theory, shows that, for an increase in the ball temperature of 43° C (110° F), the calculated shear stress drops only 35%.

The temperature model was used with Jakobsen's theory in the form of the program in Appendix B to predict the traction for Fluid N1 with a load of 67 N (15 lbs) and a sliding speed of 1.40 m/s (55 ips). The resulting traction coefficient using the iteration procedure was .052. This is compared with the calculated value, using measured temperatures, of .084, and a measured traction coefficient of .074. Based on Figure 7, the comparison would be more favorable at the higher speeds.

CHAPTER VI

CONCLUSIONS AND RECOMMENDATIONS

Summary of Conclusions

An evaluation of Jakobsen's 1973 (1) theory of traction generation applied to a sliding elastohydrodynamic contact, coupled with his proposed rheological model of the lubricant, has been performed. A computer program based on the theory was written and was used to predict the traction coefficient for several conditions of speed and load, using experimentally-determined film thickness and ball temperatures. Experimental traction measurements were made to provide a basis for comparison of the calculated results.

The theory was found to predict realistic values for the traction at high speeds. Predicted tractions were slightly lower than measured, possibly due either to shear stresses outside the Hertzian contact area, or to inaccuracies in extrapolating fluid viscosity data. The variation of traction with speed at the higher sliding velocities compared well between calculations and measurements.

However, as the speed decreased beyond a certain point, the calculated tractions significantly exceeded the measured values. One possible explanation for this disparity is that, at low speeds, the separation between bearing surfaces be-

came sufficiently small as to allow asperity interactions. This could have the effect of introducing an additional source of heat into the contact, one not taken into account by the theory. It is also possible that, as the film thickness decreases, part of the load is carried by the asperities themselves, thus decreasing the fluid pressure. This would have the effect of decreasing the viscosity and therefore the traction would decrease also.

A further possibility is the breakdown of the proposed rheological model at high shear stress. As the sliding speed decreases, the calculated shear stress was found to increase. If the fluid in reality exhibits solid-like behavior and a plastic yielding of the fluid at shear stress levels above some critical value, calculated tractions could be considerably higher than those measured.

Based on Jakobsen's theory, an evaluation of the effect on the traction of variations in the fluid parameters was performed. The traction was found to increase with an increase in base viscosity and a decrease in temperature-viscosity dependence of the lubricant. A weaker traction increase resulted from an increase in the pressure-viscosity dependence of the fluid. Variation in the thermal conductivity was found to have very little effect on the traction.

In addition, an attempt was made to make the theory applicable to engineering use by providing a means for cal-

culating film thickness and moving surface temperatures. Film thicknesses were calculated by means of Archard's point contact formula. Good correlation between calculated and measured values was found for ordinary hydrocarbon oils. For polymer-blended mineral oils, the viscosity parameters of the base oil alone should be used in the formula. Temperature calculations were based on Jaeger's formulation of the temperature distribution due to a moving source of heat. An evaluation of this formulation as applied to the EHD contact showed that the theory becomes more realistic as the sliding speed increases. Since the temperature calculation requires knowledge of the shear stress distribution, an iteration procedure must be implemented in the traction calculation. Because of the relatively mild dependence of the traction on the moving surface temperature, this procedure has been shown to give an adequate temperature distribution for the purpose of calculating traction at high speeds.

Recommendations for Further Research

Further investigation into the effects of asperity interaction and non-Newtonian lubricant behavior at high shear stress is warranted. These are two possible explanations for the discrepancy at low speeds between calculations and measurements (although other factors may be present). Therefore, it is desirable to separate the effects of these two phenomena, so that their individual contributions to the

traction may be determined. This could be accomplished by using fluids of different viscosities in the contact. A fluid with sufficiently high viscosity would result in film thicknesses large enough that the non-Newtonian effects alone could be evaluated. Conversely, a very low-viscosity fluid could result in extremely thin films at lower shear stress levels, where asperity interactions would be assured when the behavior remains Newtonian. Accurate profiles of the bearing surfaces recorded both before and after operation in the EHD contact could reveal the occurrence of interactions sufficient to alter the profile. In this way, the onset of asperity contact could be determined.

Since non-Newtonian lubricant behavior appears to occur at high shear stresses, it would be interesting to employ different rheological models with Jakobsen's theory. A composite model which is linear at low shear stress levels but becomes non-Newtonian at higher levels seems to be appropriate according to the results of this work. Further research into the existence and determination of the critical stress at which non-Newtonian behavior begins is warranted. The variation of this stress with conditions of pressure, temperature, and fluid properties is an important question which could be investigated.

There is a need for further analytical study into the traction generated outside the Hertzian contact area, particularly in the inlet region. As long as the contribution from

the Hertzian contact area alone is considered, Jakobsen's theory may be expected to yield low results for the total traction.

Improvements on the temperature model of Chapter V are needed to make it applicable to cases in which the dimensionless speed parameter is small. In its present form, the temperature model may be used in traction calculations, but its applicability to the low speed cases is open to question.

It appears, then, that the shear stress theory of Jakobsen, whether used alone or with the moving surface model based on Jaeger's formulation, is adequate for predicting the traction of sliding elastohydrodynamic contacts at high speeds. The speed at which the theory becomes applicable depends on such factors as normal load and film thickness. For the conditions of this study, realistic tractions were predicted at speeds over 2.5 m/s (100 ips). Further work is required to extend the theory to cases of lower sliding speeds, where deviations from experimental results are significant.

APPENDICES

APPENDIX A

PHYSICAL PARAMETERS OF THE EHD CONTACT

Stationary Bearing Surface

Sapphire, flat surface
Thermal Conductivity 25.1 $W/m^{o}k$ (3.14 lb $f/^{o}F$ sec)
Thermal Diffusivity 7.94×10^{-6} m^2/sec (1.23×10^{-2} in^2/sec)

Moving Bearing Surface

AISI 52100 Steel sphere, radius .625 in.
Thermal Conductivity 34.7 $W/m^{o}k$ (4.34 lb $f/^{o}F$ sec)
Thermal Diffusivity 9.56×10^{-6} m^2/sec (1.49×10^{-2} in^2/sec)
Sliding Velocity .35-12.7 m/s (13.7-500 ips)

Lubricant

Naphthenic base oil, Fluid N1 (17,18,19)
Thermal Conductivity .13 $W/m^{o}k$ (.0167 lb $f/^{o}F$ sec)
Viscosity at 38° C (100° F) 2.2×10^{-2} Ns/m^2 (22 cp)
Viscosity at 99° C (210° F) 3.2×10^{-3} Ns/m^2 (3.2 cp)

Reduced elastic modulus of bearing surfaces $E' = 2.86 \times 10^{11}$ N/m^2 (41.4×10^{6} psi)

APPENDIX B

LISTING OF FORTRAN COMPUTER PROGRAM TO CALCULATE TRACTION

The following pages contain a documented listing of the computer program used to calculate the traction coefficient of a sliding EHD point contact. The meanings of each of the major input variables are given within the body of the program, along with instructions for its use.

In its present form, the program accepts input parameters in the English system of units, as noted in the program. For convenience, Table 3 lists conversion factors for use in converting from SI units to the English units required in the program.

Table 3. Conversion Factors

Quantity	Multiply (SI)	By	To Get (English)
Length	m	39.37	in.
Pressure, shear stress	N/m^2	1.450×10^{-4}	psi
Speed	m/s	39.37	in/sec
Temperature	^{o}k	1.80	^{o}R
Thermal Conductivity	$W/m^{o}k$	.125	lb $f/^{o}F$ sec
Thermal Diffusivity	m^2/s	1550	in^2/sec
Viscosity	Ns/m^2	1×10^3	cp

```
C*****************************************************************
C    THIS PROGRAM COMPUTES THE TRACTION COEFFICIENT FOR A
C    SLIDING EHD POINT CONTACT BY CALCULATING THE SHEAR
C    STRESS AT VARIOUS LOCATIONS AND INTEGRATING OVER THE
C    CONTACT.  FILM THICKNESSES AND MOVING SURFACE TEMP-
C    ERATURES MAY EITHER BE INPUT OR CALCULATED.
C    ***NOTE***INPUT VARIABLES AND THEIR UNITS DEFINED BEFORE
C    EACH READ STATEMENT.  SPECIAL NOTES:
C      * PROVIDE DATA ONLY IF BALL TEMP. TO BE CALCULATED
C      & PROVIDE DATA ONLY IF FILM THICKNESS TO BE CALCULATED
C*****************************************************************
      DIMENSION Y(30),TINT(30),YY(3),XX(3)
      H=0.0
      T2=0.0
      REAL KT,KTB,L
C    SET NT=0 IF NO BALL TEMP. DATA PROVIDED; =1 OTHERWISE
C    SET NH=0 IF NO FILM THICKNESS DATA PROVIDED; =1 OTHERWISE
      READ(5,350)NT,NH
C    T1LF,T2SF: TEMPERATURES AT WHICH VISCOSITIES ARE
C      PROVIDED (R)
C    KT: THERMAL CONDUCTIVITY OF FLUID (LB/SEC-F)
C    KTB: THERMAL CONDUCTIVITY OF BALL (LB/SEC-F)
C    DIFF: THERMAL DIFFUSIVITY OF BALL (IN-IN/SEC)
      READ(5,350)T1LF,T2SF,KT,KTB,DIFF
C    UH: SLIDING SPEED (IN/SEC)
C    M1: NO. OF LINES ALONG WHICH CALCULATIONS ARE
C      TO BE MADE
C    L: NORMAL LOAD(LBF)
C    R: REDUCED ROLLER RADIUS (IN)
      READ(5,350)UH,M1,L,R
      IF(NH.EQ.1)GO TO 20
C   &ALPH: BASE VISCOSITY AT INLET TEMP.(CP)
C   &ETA: BASE VISCOSITY AT INLET TEMP. (CP)
C   &ALPH: PRESSURE-VISCOSITY COEFFICIENT AT INLET TEMP(1/PSI)
C   &ED: REDUCED ELASTIC MODULUS OF SURFACES (PSI)
C   &PHZ: MAX. HERTZ PRESSURE IN CONTACT (PSI)
      READ(5,350)ALPH,ETA,ED,PHZ
      G=ALPH*ED
      U=(ETA*UH)/(2.*ED*R*6895000.)
      P=PHZ/ED
      H=1.37*R*(G**.74)*(U**.74)/(P**.22)
   20 IF(NT.EQ.1)GO TO 21
C   *T2: INLET BALL TEMPERATURE (R)
      READ(5,350)T2
   21 WRITE(6,901)UH,KT,T1LF,KTB,T2SF,DIFF,L,R
  901 FORMAT(//' UH = ',F10.2,' IN/SEC',7X,'KT = ',F10.4,
     1' LB/SEC-F'/
```

```
     2' T1LF = ',F10.2,' R',10X,'KTB = ',F10.4,' LB/SEC-F'/
     3' T2SF = ',F10.2,' R',10X,'DIFF = ',F10.4,' IN-IN/SEC'/
     4' LOAD = ',F10.1,' LBF', 8X,'HERTZIAN RADIUS = ',
     5F7.4,' IN.'/)
      M=M1+1
C    CALL SUBROUTINE FOR EVALUATING SHEARS ALONG LINE AND
C    INTEGRATING IN X1-DIRECTION
      DO 22 I=2,M
      CALL LINE(T1LF,T2SF,KT,KTB,DIFF,UH,T2,H,Y(I),TINT(I),R)
   22 CONTINUE
C    PERFORM INTEGRATION IN X2-DIRECTION, TAKING THREE
C    POINTS AT A TIME, AND SUMMING INTEGRATED RESULTS
      TRAC=0.0
      Y(1)=0.0
      TINT(1)=0.0
      DO 23 I=1,M1
      TINT(2*M-I)=TINT(I)
      Y(2*M-I)=2.0*R-Y(I)
   23 CONTINUE
      DO 24 I=1,M1
      DO 25 J=1,3
      LL=2*I-2+J
      XX(J)=Y(LL)
      YY(J)=TINT(LL)
   25 CONTINUE
      Y1=(YY(2)-YY(1))/(XX(2)-XX(1))
      Y2=(YY(3)-YY(2))/(XX(3)-XX(2))
      Y3=(Y2-Y1)/(XX(3)-XX(1))
      A=Y3
      B=Y1-(XX(1)+XX(2))*Y3
      C=YY(1)-XX(1)*Y1+XX(1)*XX(2)*Y3
      DTR=(A/3.)*(XX(3)**3-XX(1)**3)+(B/2.)*(XX(3)**2-
     1XX(1)**2)+C*(XX(3)-XX(1))
       TRAC=TRAC+DTR
   24 CONTINUE
      TC=(TRAC/L)*100.
      WRITE(6,100) TC
  100 FORMAT(/////15X,'TRACTION COEFFICIENT = ',F10.3,
     1' PER CENT'//)
  350 FORMAT()
      STOP
      END
```

```
      SUBROUTINE LINE(T1LF,T2SF,KT,KTB,DIFF,UH,T2,H2,Y,
     1TINT,R)
C*****************************************************************
C    THIS SUBROUTINE READS IN DATA FOR A LINE OF POINTS IN
C    THE CONTACT, AND INTEGRATES THE SHEAR STRESS ALONG THIS
C    LINE (IN X1-DIRECTION)
C    DATA FOR THIS SUBROUTINE MUST BE PROVIDED FOR EACH
C    LINE CALCULATED..
C    ***NOTE***INPUT VARIABLES AND THEIR UNITS DEFINED BEFORE
C    EACH READ STATEMENT.  SPECIAL NOTES:
C      * PROVIDE DATA ONLY IF BALL TEMP. TO BE CALCULATED
C      # PROVIDE DATA ONLY IF BALL TEMP. MEASURED
C      & PROVIDE DATA ONLY IF FILM THICKNESS TO BE CALCULATED
C      + PROVIDE DATA ONLY IF FILM THICKNESS MEASURED
C*****************************************************************
      REAL KT,KTB
      DIMENSION DIFT(30),DIFF2(30)
C    N: NO. OF POINTS IN LINE TO BE CALCULATED
C    Y1: DISTANCE OF LINE FROM CENTERLINE (IN)
C    DELX: DISTANCE BETWEEN POINTS (IN)
      READ(5,350)N,Y1,DELX
      DIMENSION MM(30)
      DIMENSION X(30),H(30),T2S(30),TAU(30),CPS(30),CPL(30)
      DIMENSION TAPP(30),H1(30)
      DIMENSION Q(30),E(30),TFT1L(30),TFT2S(30),TAPP2(30)
      WRITE(6,551)Y1
  551 FORMAT(/////9X,'COMPUTED ON A LINE ',F7.4,' IN. FROM
     1 CENTERLINE.')
      N1=N-1
C    X(I): NUMBER OF POINT I
C    CPS(I): VISC. AT PRESSURE OF PT. I, TEMP.T1LF (CP)
C    CPL(I): VISC. AT PRESSURE OF PT. I, TEMP.T2SF(CP)
      READ(5,350)(X(I),CPS(I),CPL(I),I=2,N1)
      Y=R-Y1
C    IF FILM THICKNESS NOT INPUT, GO TO 90
      IF(H2.GT.0.0)GO TO 90
C   +H(I): MEASURED FILM THICKNESS AT POINT I (IN)
      READ(5,350)(H(I),I=2,N1)
      GO TO 91
   90 DO 92 I=2,N1
      H(I)=H2
   92 CONTINUE
C    IF BALL TEMPS. INPUT, GO TO 65; OTHERWISE START
C    ITERATION PROCESS
   91 IF(T2.LE.0.0)GO TO 65
C   *TAPP(I): ESTIMATED SHEAR STRESS AT PT. I (PSI)
      READ(5,350)(TAPP(I),I=1,N)
```

```
      T2S(1)=T2
      TAU(1)=0.0
      TAU(N)=0.0
      LM=0
      TAV2=0.0
      DO 61 I=2,N1
      DIFF2(I)=10.**6
   61 CONTINUE
      NN=0
C     CALL SUBROUTINE TO CALCULATE BALL TEMPS. BASED ON TAPP
   20 CALL MOTEM(TAPP,T2,DELX,N,KTB,DIFF,UH,T2S)
      GO TO 66
C    #T2S(I): MEASURED BALL TEMP. AT PT. I (R)
   65 READ(5,350)(T2S(I),I=2,N1)
C     FOR EACH POINT CALL SUBROUTINE TO FIND SHEAR STRESS
   66 DO 10 I=2,N1
      CALL SHEAR(CPS(I),T1LF,CPL(I),T2SF,KT,H(I),UH,T2S(I),
     1TAU(I),I,Q(I),E(I),TFT1L(I),TFT2S(I))
   10 CONTINUE
C     PERFORM INTEGRATION IN X1-DIRECTION - SIMPSON'S METHOD
      YE=0.0
      YO=0.0
      DO 12 I=2,N1,2
      YE=YE+TAU(I)
   12 CONTINUE
      N2=N-2
      DO 15 I=3,N2,2
      YO =YO+TAU(I)
   15 CONTINUE
      TAV=1./(3.*(N-1))*(4.*YE+2.*YO)
      TINT=(DELX/3.)*(4.*YE+2.*YO)
C     IF TEMPERATURES WERE PROVIDED, GO TO PRINT SECTION;
C     OTHERWISE CONTINUE ITERATION PROCESS
      IF(T2.LE.0.0)GO TO 31
      DTAV=ABS(TAV2-TAV)/TAV
C     TEST FOR CONVERGENCE OF AVERAGE SHEAR(DTAV)
      IF(DTAV.LT.0.002)LM=LM+1
      IF(LM.EQ.0)GO TO 25
      WRITE(6,550)
  550 FORMAT(//5X,'AVE. TAU STABLE. TAPP GIVEN BELOW')
      WRITE(6,350)(TAPP(I),I=2,N1)
      GO TO 31
   25 NV=0
C     TEST FOR CONVERGENCE OF SHEAR AT EACH POINT
      DO 30 I=2,N1
      IF(TAPP(I).LE.0.0)GO TO 29
      DIFT(I)=ABS((TAPP(I)-TAU(I))/TAPP(I))
      IF(DIFT(I).LT.0.05)GO TO 30
   29 NV=NV+1
   30 CONTINUE
```

```
      IF(NV.GT.0)GO TO 40
C   PRINT FINAL DISTRIBUTIONS ALONG THE LINE
   31 WRITE(6,905)
  905 FORMAT(//5X,'FINAL DISTRIBUTIONS ALONG LINE'//)
      WRITE(6,900)
  900 FORMAT(2X,'LOCN',7X,'Q',4X,'E (R)',3X,'T1 (F)',3X,
     1'T2 (F)',2X,'H (UIN)',2X,'TAU (PSI'/)
      DO 59 I=2,N1
      H1(I)=(10.**6)*H(I)
      WRITE(6,904)I,Q(I),E(I),TFT1L(I),TFT2S(I),H1(I),TAU(I)
  904 FORMAT(2X,I3,5X,F6.3,2X,F5.0,3X,F5.1,4X,F5.1,3X,F5.1,
     14X,F7.0)
   59 CONTINUE
      WRITE(6,702)TAV
  702 FORMAT(///5X,'AVERAGE SHEAR = ',F10.2,'  PSI')
      WRITE(6,703) TINT
  703 FORMAT(/5X,'LINE INTEGRAL = ',F10.2,'  LBF/IN')
   21 RETURN
C   C   IF 10 ITERATIONS PERFORMED, EXIT
   40 IF(NN.GT.9)GO TO 50
   71 WRITE(6,701)TAV
  701 FORMAT(//5X,'CALCULATED AVE. TAU',1PE11.5,'PSI'/)
      WRITE(6,710)TINT
  710 FORMAT(5X,'INTEGRAL OVER THE LINE = ',1PE11.5,
     1' LBF/IN'/)
      WRITE(6,721)
  721 FORMAT(5X,'INSUFFICIENT CONVERGENCE.  ALTER TAPP'//)
C   AD HOC PROCEDURE FOR UPDATING TAPP TO FACILITATE
C   CONVERGENCE
   16 DO 41 I=2,N1
      IF(NN.LT.5)GO TO 42
      IF(DIFT(I).GT.0.05)GO TO 51
      IF(MM(I).NE.1)GO TO 53
      TAPP(I)=TAPP2(I)
      GO TO 41
   53 IF(DIFT(I).LT.DIFF2(I))GO TO 42
      DIFT(I)=DIFF2(I)
      TAPP(I)=TAPP2(I)
      GO TO 41
   51 IF(DIFT(I).LT.DIFF2(I))GO TO 42
      IF(DIFF2(I).GT.0.05)GO TO 47
      MM(I)=1
      TAPP(I)=TAPP2(I)
      GO TO 41
   47 A=TAPP(I)
      TAPP(I)=.50*(TAPP(I)+TAPP2(I))
      TAPP2(I)=A
      GO TO 41
   42 TAPP2(I)=TAPP(I)
      TAPP(I)=.20*TAPP(I)+.80*TAU(I)
```

```
   41 CONTINUE
   43 TAPP(1)=0.0
      TAPP(N)=0.0
      NN=NN+1
      DO 18 I=2,N1
      DIFF2(I)=DIFT(I)
   18 CONTINUE
      TAV2=TAV
C    IF CONVERGENCE NOT ACHIEVED, RETURN FOR ANOTHER ITERATION
      GO TO 20
   50 WRITE(6,730)
  730 FORMAT(//5X,'CONVERGENCE INCOMPLETE AFTER 10'
     1' ITERATIONS.  TAPP GIVEN BELOW.')
      WRITE(6,350)(TAPP(I),I=2,N1)
      GO TO 31
  350 FORMAT()
      END


      SUBROUTINE MOTEM(TAU,TAMB,DELX,N,KTB,DIFF,UH,T)
C*****************************************************************
C    SUBROUTINE FOR CALCULATING MOVING SURFACE TEMP.,T,
C    BY SETTING UP SHEAR STRESS SEGMENTS BASED ON TAU. THEY
C    ARE SET UP BY MOVING FROM INLET TO OUTLET, CREATING OR
C    TERMINATING ALL OR PART OF A SEGMENT DEPENDING ON
C    WHETHER SHEAR IS INCREASING OR DECREASING AT THAT POINT.
C    J IS THE NUMBER OF THE POINT CURRENTLY UNDER CONSIDERA-
C    TION.  WE TRY TO FIND THE TEMPERATURE AT J DUE TO THE
C    UPSTREAM SHEAR.
C*****************************************************************
      DIMENSION TAU(30),M(30),TT(30),CD(30),CA(30)
      DIMENSION DELT(30),T(30)
      REAL KTB
      C=(2./KTB)*SQRT(DIFF*UH/3.14159)
      L=0
      SUMT=0.0
      KK=0
      T(1)=TAMB
      DO 200 J=2,N
      IF(TAU(J).LT.TAU(J-1))GO TO 20
C    SET UP A NEW SEGMENT
      KK=KK+1
      M(KK)=1
C    HEIGHT OF SEGMENT NO. KK IS TT
      TT(KK)=0.5*(TAU(J-1)+TAU(J))-SUMT
      SUMT=SUMT+TT(KK)
C    CD(KK) IS DISTANCE FROM J TO BEGINNING OF SEGMENT KK
C    CA(KK) IS DISTANCE FROM J TO END OF SEGMENT KK
      CD(KK)=0.0
      CA(KK)=0.0
```

```
      L=KK
      LL=1
      GO TO 100
   20 IF(TAU(J).GT.SUMT)GO TO 80
C   DECIDE WHETHER TO END ALL OR PART OF TOP SEGMENT,
C   DEPENDING ON VALUE OF TAU(J)
      IF((SUMT-TAU(J)).LT.(0.33*TT(L)))GO TO 30
      IF((SUMT-TAU(J)).LT.(0.75*TT(L)))GO TO 40
C   END TOP SEGMENT AT A LOCATION BETWEEN POINT J AND J-1
      S=(TAU(J-1)-TAU(J))/DELX
      X=(TAU(J-1)-SUMT+0.5*TT(L))/S
      CA(L)=-1.0*X
      M(L)=0
      SUMT=SUMT-TT(L)
      DO 51 I=L,1,-1
      IF(M(I).EQ.1)L=I
      IF(M(I).EQ.1)GO TO 52
   51 CONTINUE
      GO TO 200
C   CHECK TO SEE IF NEXT SEGMENT SHOULD BE ENDED
   52 IF(SUMT.GT.TAU(J))GO TO 20
      GO TO 100
   30 IF(TAU(J+1).GT.TAU(J))GO TO 100
      KK=KK+1
      IF((KK-L).EQ.1)GO TO 32
      L1=L+2
      DO 31 I=KK,L1,-1
      TT(I)=TT(I-1)
C   END ENTIRE TOP SEGMENT
      CD(I)=CD(I-1)
      CA(I)=CA(I-1)
      M(I)=M(I-1)
   31 CONTINUE
C   END HALF OF NEXT SEGMENT
   32 TT(L+1)=0.5*TT(L)
      M(L+1)=0
      CA(L+1)=-1.0*DELX
      CD(L+1)=CD(L)
      TT(L)=0.5*TT(L)
      SUMT=SUMT-TT(L+1)
      LL=1
      GO TO 100
   40 IF(TAU(J+1).GT.TAU(J))GO TO 100
      CA(L)=-1.0*DELX
      M(L)=0
      SUMT=SUMT-TT(L)
      L=L-1
      DO 42 I=L,0,-1
      IF(M(I).EQ.1)L=I
      IF(M(I).EQ.1)GO TO 41
```

```
   42 CONTINUE
   41 LL=0
      GO TO 100
   80 IF(LL.EQ.0)GO TO 100
C    ADD ON ANOTHER SMALL SEGMENT
      IF((TAU(J)-SUMT).LT.(0.25*TT(L+1)))GO TO 100
      SUMT=SUMT+0.5*TT(L+1)
      TT(L)=TT(L)+0.5*TT(L+1)
      TT(L+1)=0.5*TT(L+1)
  100 DELT(J)=0.0
C    SUM CONTRIBUTIONS OF EACH SEGMENT TO DETERMINE TEMP.
      DO 110 I=1,KK
      CD(I)=CD(I)+DELX
      IF(M(I).EQ.0)CA(I)=CA(I)+DELX
      DELT(J)=DELT(J)+C*TT(I)*(SQRT(CD(I))-SQRT(CA(I)))
  110 CONTINUE
      T(J)=TAMB+DELT(J)
  200 CONTINUE
      RETURN
      END


      SUBROUTINE SHEAR(CPS,T1LF,CPL,T2SF,KT,H,UH,T2S,TAU,
     1I,Q,E,TFT1L,TFT2S)
C*****************************************************************
C    THIS SUBROUTINE COMPUTES THE SHEAR STRESS AT A  POINT
C    BY NUMERICALLY INTEGRATING JAKOBSEN'S FORMULA FOR
C    THE ADIABATIC WALL CASE
C*****************************************************************
      DIMENSION DT(305),DREYH(305),DDSU(305),DSU(305)
      DIMENSION VRDSU(305),DDSSU(305),DSSU(305)
      DIMENSION RIOV(305),TVOV(305)
      REAL KT
      Q=(ALOG((ALOG(CPS))/(ALOG(CPL))))/(ALOG((T2SF)/(T1LF)))
      A=(ALOG(CPS))*(T1LF)**Q
      E=A**(1./Q)
      C1=1./6895000.
      PI2=T2S/E
      CALL DETEMP(1,PI2,Q,.150,D)
      PI4=C1*UH*UH/(2.*KT*E)
      D=D+PI4
      CALL DETEMP(2,PI1,Q,.150,D)
      T1L=PI1*E
      PI3=Q
      DDELTA=(PI1-PI2)/100.
      DDEL=DDELTA
      DT(1)=PI2
      DSU(1)=0.0
      VRDSU(1)=1./((PI4)**.5)
      DSSU(1)=0.0
```

```
      DREYH(1)=EXP((1./DT(1))**PI3)
      DO 50 J=2,300
      DT(J)=DT(J-1)+DDEL
      IF(DT(J).GT.PI1)GO TO 21
      DREYH(J)=EXP((1./DT(J))**PI3)
      DDSU(J-1)=(2.*DDEL)/(DREYH(J)+DREYH(J-1))
      DSU(J)=DDSU(J-1)+DSU(J-1)
      IF(DSU(J).GE.PI4)GO TO 21
      VRDSU(J)=1./((PI4-DSU(J))**.5)
      DDSSU(J-1)=(DDEL/2.)*(VRDSU(J)+VRDSU(J-1))
      DSSU(J)=DDSSU(J-1)+DSSU(J-1)
      RIOV(J)=(VRDSU(J)-VRDSU(J-1))
      TVOV(J)=.05*VRDSU(J-1)
      DDELT=.05*DDELTA
      DDELTT=.01*DDELTA
C   DECREASE STEPSIZE AS CURVE STEEPENS
      IF(DDEL.LT.(.5*DDELT))GO TO 51
      IF(RIOV(J).GT.TVOV(J))DDEL=DDELT
      IF(RIOV(J).GT.(2.*TVOV(J)))DDEL=DDELTT
   51 PI5=(DSSU(J))/(2.*((DSU(J))**.5))
   50 CONTINUE
   21 TAU=PI5*UH*C1/H
      TFT2S=T2S-459.67
      TFT1L=T1L-459.67
      RETURN
      END


      SUBROUTINE DETEMP(N,PI,PI3,PI0,D)
C*****************************************************************
C   THIS SUBROUTINE COMPUTES THE INTEGRAL OF THE INVERSE
C   VISCOSITY FUNCTION FROM PI0 TO PI, IN STEPS OF DDEL
C*****************************************************************
      DIMENSION DT(305),DREYH(305),DDSU(305),DSU(305)
      PM=(1./PI0)**PI3
      IF(PM.LT.87.5)GO TO 15
      PI0=EXP(-4.47/PI3)
   15 DDEL=.0025
      DT(1)=PI0
      DSU(1)=0.0
      DREYH(1)=EXP((1./DT(1))**PI3)
      DO 10 J=2,300
C   INCREASE STEP AS CURVE LEVELS OFF
      IF(J.GT.81)DDEL=.005
      DT(J)=DT(J-1)+DDEL
      DREYH(J)=EXP((1./DT(J))**PI3)
      DDSU(J-1)=(2.*DDEL)/(DREYH(J)+DREYH(J-1))
      DSU(J)=DDSU(J-1)+DSU(J-1)
```

```
C     IF N=2 AND VALUE OF INTEGRAL=D, THEN RETURN
        IF(N.EQ.2)GO TO 5
        IF(DT(J).LT.PI)GO TO 10
        D=DSU(J-1)+((DSU(J)-DSU(J-1))*(PI-DT(J-1)))/(DT(J)-
       1DT(J-1))
        RETURN
C     IF N=1 AND UPPER LIMIT IS REACHED, RETURN
    5   IF(DSU(J).LT.D)GO TO 10
        PI=DT(J-1)+((DT(J)-DT(J-1))*(D-DSU(J-1)))/(DSU(J)-
       1DSU(J-1))
        RETURN
   10 CONTINUE
        WRITE(6,400)
  400 FORMAT(5X,'LIMIT EXCEEDED.  INCREASE PI0')
        STOP
        END
```

APPENDIX C

SAMPLE COMPUTER OUTPUT

The following is a typical set of output from the computer program of Appendix B. Computations were made for Fluid N1 at a sliding speed of 2.54 m/s (100 ips) and a normal load of 67 N (15 lb). Measured values of film thickness and moving surface temperature were used. In addition to the traction coefficient, values for Q,E, surface temperatures, film thickness, and shear stress are given for each point at which calculations are made.

```
UH =      100.00 IN/SEC        KT =        .0167 LB/SEC-F
T1LF =      669.67 R           KTB =      4.3400 LB/SEC-F
T2SF =      559.67 R           DIFF =       .0149 IN-IN/SEC
LOAD =        15.0 LBF         HERTZIAN RADIUS =    .0070 IN.

>@ADD N1.PL1
```

COMPUTED ON A LINE .0050 IN. FROM CENTERLINE.

FINAL DISTRIBUTIONS ALONG LINE

LOCN	Q	E (R)	T1 (F)	T2 (F)	H (UIN)	TAU (PSI)
2	3.137	1239.	224.1	145.2	5.2	3634.
3	3.044	1352.	269.4	153.7	5.2	4954.
4	3.014	1402.	290.4	164.3	5.2	5341.
5	2.989	1442.	306.5	176.1	5.2	5502.
6	2.985	1451.	310.6	186.9	5.2	5334.
7	2.989	1442.	306.8	195.6	5.2	4873.
8	3.014	1402.	291.4	202.9	5.2	4077.
9	3.044	1352.	272.0	206.9	4.4	3789.
10	3.137	1239.	236.3	207.5	4.8	1751.

AVERAGE SHEAR = 3959.46 PSI

LINE INTEGRAL = 39.59 LBF/IN

COMPUTED ON A LINE .0000 IN. FROM CENTERLINE.

FINAL DISTRIBUTIONS ALONG LINE

LOCN	Q	E (R)	T1 (F)	T2 (F)	H (UIN)	TAU (PSI)
2	3.086	1296.	246.6	142.8	7.8	3025.
3	2.993	1437.	304.5	155.1	7.0	4568.
4	2.957	1511.	336.1	171.1	7.1	4898.
5	2.938	1557.	355.7	187.8	7.0	5072.
6	2.929	1585.	368.0	205.2	7.0	4986.
7	2.923	1603.	375.6	221.2	7.0	4762.
8	2.919	1613.	380.2	235.2	7.0	4572.
9	2.923	1603.	375.8	245.4	7.0	4177.
10	2.929	1585.	368.5	254.2	7.1	3723.
11	2.938	1557.	356.9	260.0	7.2	3228.
12	2.957	1511.	338.5	261.1	7.7	2521.
13	2.993	1437.	310.8	258.8	7.7	1835.
14	3.086	1296.	271.8	252.8	8.7	672.

AVERAGE SHEAR = 3449.43 PSI

LINE INTEGRAL = 48.29 LBF/IN

TRACTION COEFFICIENT = 4.220 PER CENT

APPENDIX D

FILM THICKNESS CALCULATIONS FOR VARIOUS FLUIDS

Film thickness calculations based on Archard's equation (8) were made for various lubricants for several conditions of load and speed. Table 4 gives a description of each fluid, the references from which data on the fluid was obtained, and the fluid's designation, both in the original references and in this work.

Figures 8-11 show calculated values compared to the measured centerline film thicknesses under the same load and speed conditions. In a given figure, different data points for a single fluid correspond to different sliding speeds.

Table 4. Fluid Descriptions

Designation	Reference	Description
3	34	Octylmethyl siloxane
6	34	Decylmethyl siloxane
7	34	Tetradecylmethyl siloxane
8	34	Hexylmethyl siloxane
12	34	Dimethyl siloxane
14	34	Methyl-phenyl
I	34	Fluorosilicone
N1	17	Naphthenic base oil
N2	17	N1 + 4% Polyalkylmethacrylate (PL4521)
N3	17	N1 + 4% Polyalkylmethacrylate (PL4523)
S1	17	Diester
S2	17	Polybutene
S3	17	Dimethyl siloxane
S4	17	Trifluoropropylmethyl siloxane
P1	17	Paraffinic bas oil
P2	17	P1 + 4% Polyalkylmethacrylate
P3	17	P1 + 8% Polyalkylmethacrylate
P4	17	P1 + 18% Polybutene
P5	17	P1 + 4.4% Polybutene
A	35	Advanced ester
B	35	Formulated advanced ester
DN600	35	Polyalkyl aromatic
D	35	Synthetic paraffinic oil + additive
C	35	Naphthenic mineral oil + additive
MCS460	35	Synthetic hydrocarbon
MCS418	35	Modified polyphenyl ether

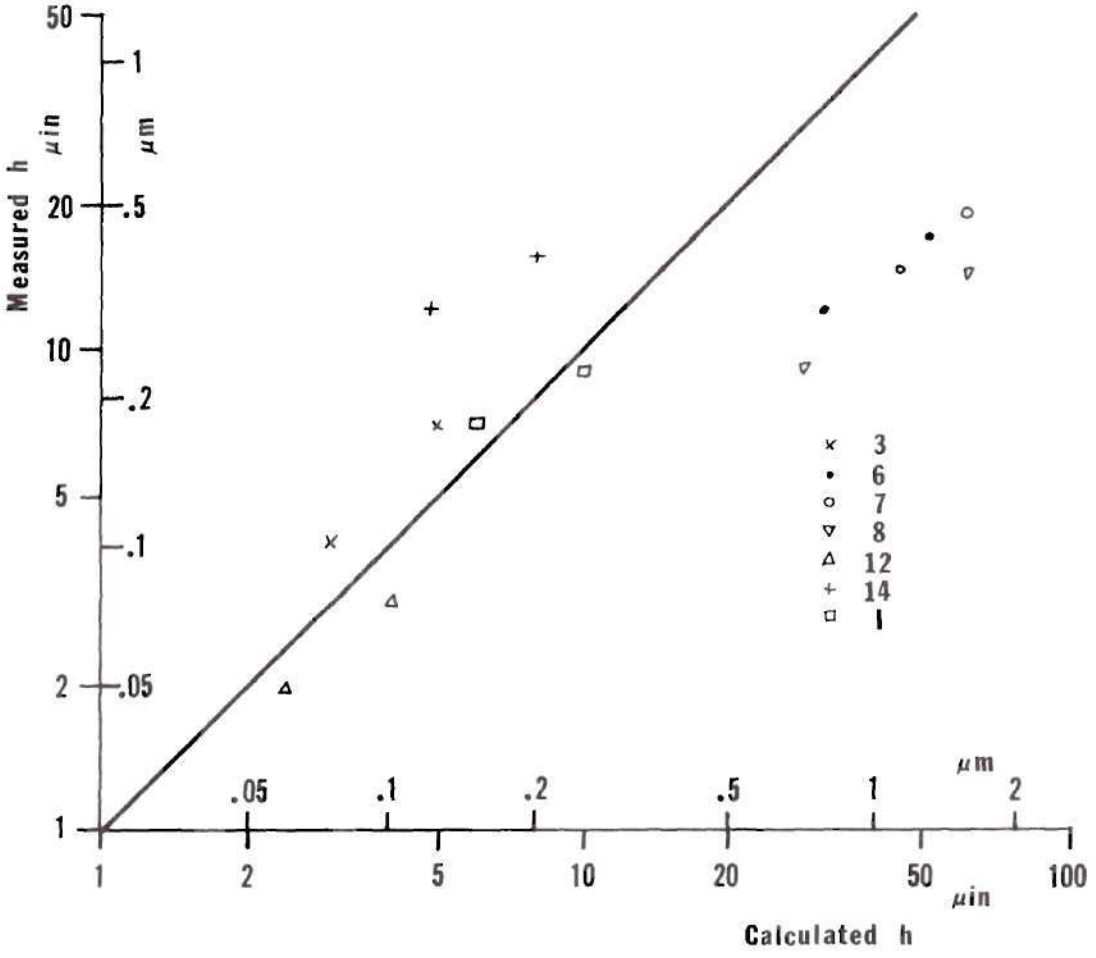

Figure 8. Results of Film Thickness Calculations - I.

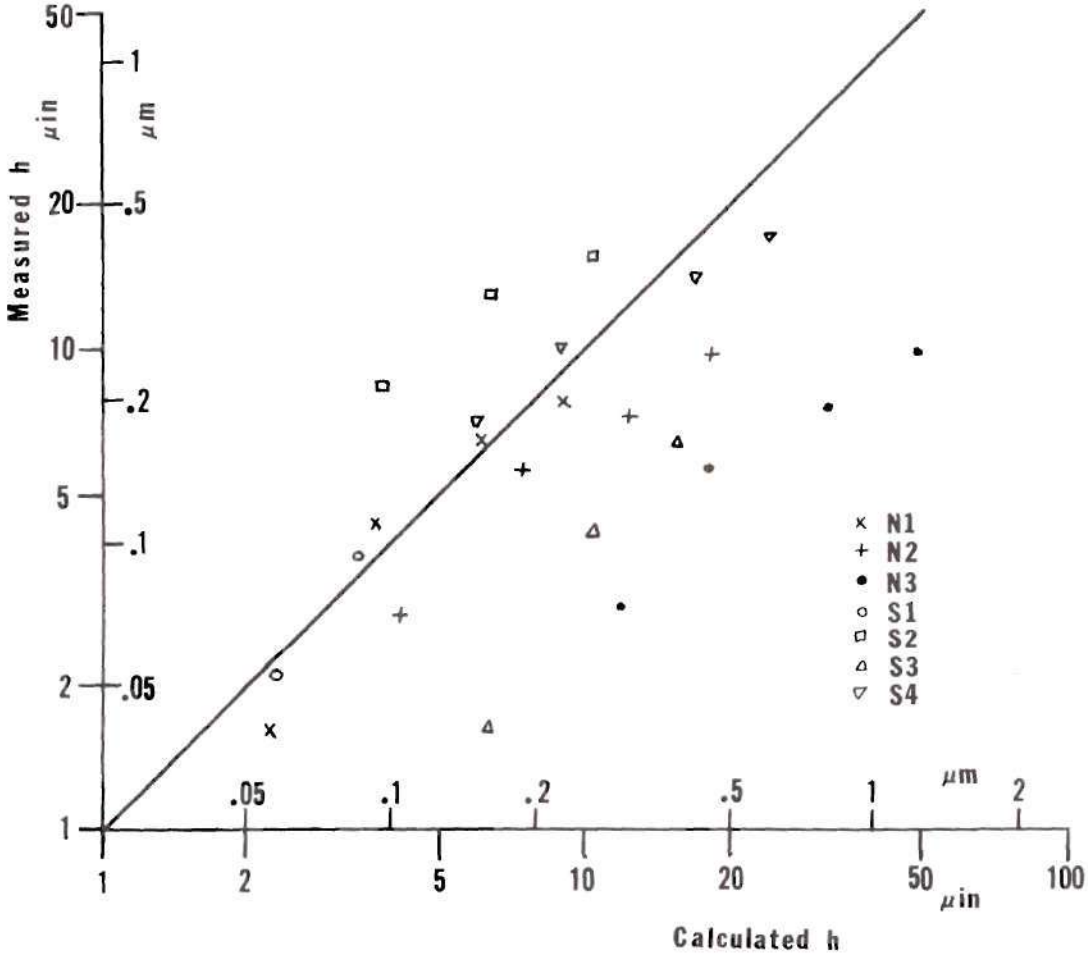

Figure 9. Results of Film Thickness Calculations - II.

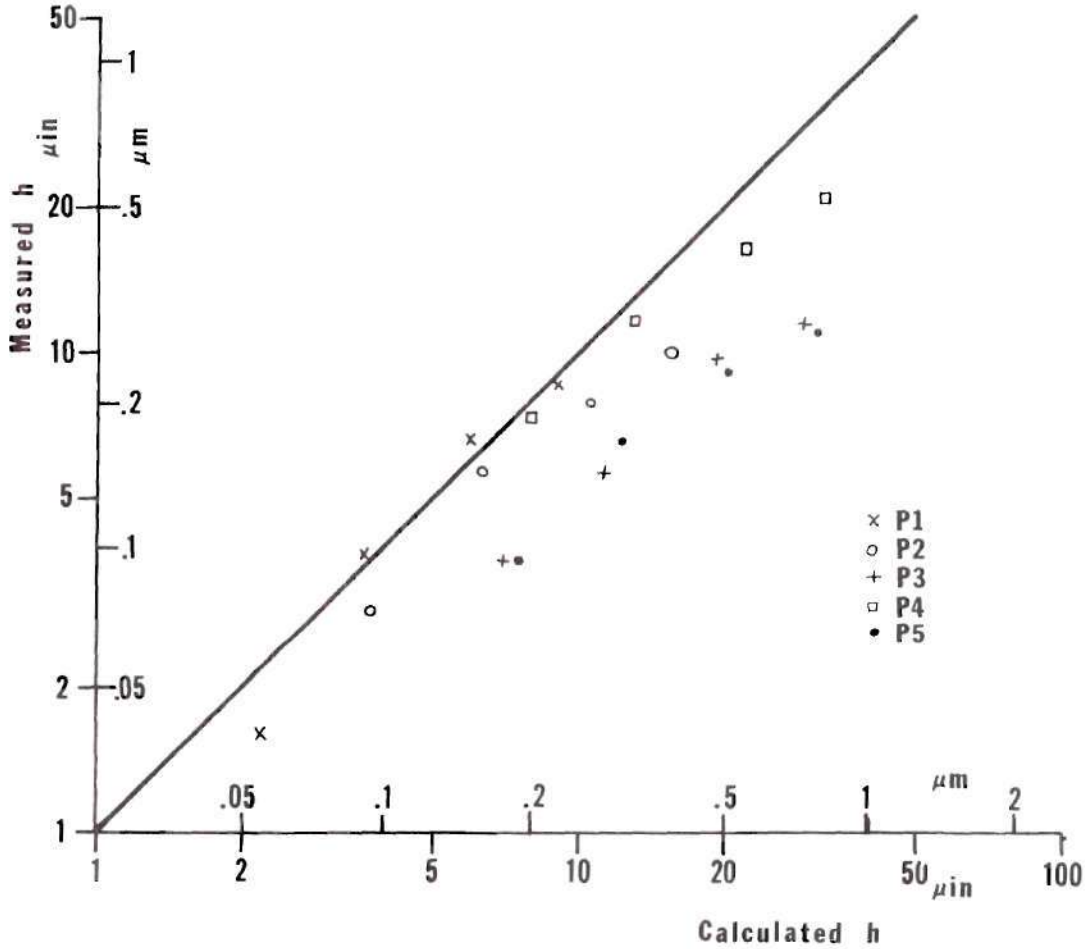

Figure 10. Results of Film Thickness Calculations - III.

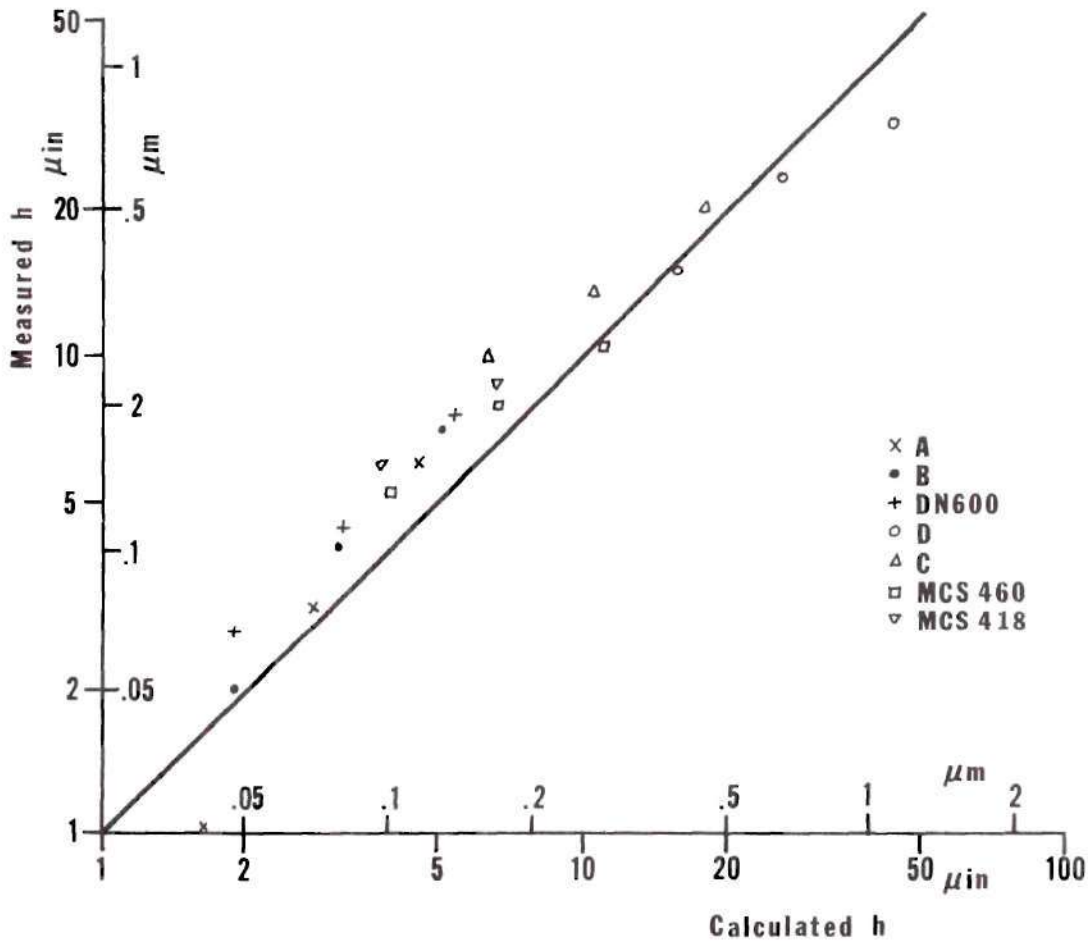

Figure 11. Results of Film Thickness Calculations - IV.

APPENDIX E

NOMENCLATURE

Symbol	Description
a	Radius of Hertzian contact
c_1	Dimensioned constant $(\eta/\lvert\eta\rvert)$
E	Material parameter in power-exponential viscosity relation
E'	Reduced elastic modulus of contact materials
G	Dimensionless material parameter in Archard's formula $(\alpha E')$
h	Film thickness
k	Thermal conductivity of lubricant
k_{tb}	Thermal conductivity of ball (moving surface)
ℓ	Length of moving heat source
p	Pressure
p_{hz}	Maximum Hertz pressure in the contact
P_{hz}	Dimensionless load parameter in Archard's formula $(\frac{p_{hz}}{E'})$
q	Strength of moving heat source (energy/unit time/unit area)
Q	Temperature-viscosity coefficient in power-exponential relation $(= \pi_3)$
r	Distance from center of contact

Symbol	Description
R	Reduced roller radius (equal to ball radius)
T	Temperature
T_1	Temperature of stationary surface
T_2	Temperature of moving surface
TC	Traction coefficient
Tr	Traction force
U	Dimensionless speed parameter in Archard's formula $(\frac{\eta_o (UH)}{2\ E'\ R})$
u_1, u_2, u_3	Velocities in x_1, x_2, x_3 directions
UH	Sliding speed
V	Jaeger's dimensionless speed parameter $(\frac{(UH)\ \ell}{2\ \kappa})$
x	Distance from leading edge of heat source
x_1, x_2, x_3	Coordinates in Cartesian coordinate system
Z	Roelands' pressure-viscosity coefficient
α	Exponential pressure-viscosity coefficient
α^*	Pressure-viscosity coefficient obtained from the Weibull transformation $\left[\eta_o \int_o^\infty \frac{dp}{\eta(p)}\right]^{-1}$
ΔT_2	Temperature rise above inlet of point on moving surface
η	Viscosity
η_o	Viscosity at atmospheric pressure
θ	Dimensionless temperature (T/E)
κ	Thermal diffusivity of moving surface
λ	Composite rms peak-to-valley surface roughness

Symbol	Description
μ	Dimensionless viscosity (η/c_1)
ξ	Dummy variable of dimensionless temperature
π_o	Arbitrary dimensionless temperature ($\pi_o << \pi_2$)
π_1	Dimensionless stationary surface temperature (T_1/E)
π_2	Dimensionless moving surface temperature (T_2/E)
π_3	Dimensionless temperature-viscosity coefficient (Q)
π_4	Dimensionless velocity parameter ($c_1(UH)^2/2kE$)
π_5	Dimensionless shear stress parameter ($\tau h/c_1(UH)$)
ρ	Density
τ	Shear stress
ϕ_T	Thermal reduction factor

BIBLIOGRAPHY

1. Jakobsen, J., "Lubricant Rheology at High Shear Stress", Ph.D. Dissertation, Georgia Institute of Technology, September 1973.

2. Jakobsen, J. and Winer, W. O., "Traction of Elastohydrodynamic Contacts with Thermal Shearing Flows", ASME Paper No. 74-LUB-28.

3. Cheng, H. S., "Application of Elastohydrodynamics to Rolling Element Bearings", ASME paper # 74-DE-32.

4. Crook, A. W., "The Lubrication of Rollers III: A Theoretical Discussion of Friction and Temperature in the Film", Phil. Trans. Roy. Soc. of London, A, 254, 1961.

5. Kannel, J. W. and Walowit, J. A., "Simplified Analyses for Tractions between Rolling-Sliding EHD Contacts", Trans ASME, Journal of Lubrication Technology, Series F, Vol. 93, No. 1, 1971.

6. Allen, C. W., Townsend, D., and Zaretsky, E., "Elastohydrodynamic Lubrication of a Spinning Ball in a Non-Conforming Groove", Trans ASME, Journal of Lubrication Technology, Series F, Vol. 93, No. 1, 1970.

7. Turchina, V., Sanborn, D. M., and Winer, W. O., "Temperature Measurements in Sliding Elastohydrodynamic Point Contacts", Trans. ASME, Journal of Lubrication Technology, Series F, Vol. 96, No. 3, 1974.

8. Cheng, H. S. and Sternlicht, B., "A Numerical Solution for the Pressure, Temperature, and Film Thickness between Two Infinitely Long, Lubricated, Rolling and Sliding Cylinders under Heavy Loads", Trans. ASME, Journal of Basic Engineering, Series D, Vol. 87, No. 3, 1965.

9. Chen, H. S., "A Refined Solution to the Thermal-Elastohydrodynamic Lubrication of Rolling and Sliding Cylinders", ASLE Trans., Vol. 8, No. 4, 1965.

10. Smith, F. W., "The Effect of Temperature in Concentrated Contact Lubrication", ASLE Trans., Vol. 5, No. 2, 1962.

11. Crook, A. W., "The Lubrication of Rollers IV: Measurements of Friction and Effective Viscosity", Phil. Trans. of Roy. Soc. of London, A, Vol. 254, 1963.

12. Dyson, A., "Frictional Traction and Lubricant Rheology in Elastohydrodynamic Lubrication", Phil. Trans. of Roy. Soc. of London, A, Vol. 266, 1970.

13. Dowson, P. and Higginson, G. R., Elastohydrodynamic Lubrication, Pergamon Press, N. Y., 1966.

14. Archard, J. F. and Baglin, K. P., "Non-dimensional Presentation of Frictional Tractions in Elastohydrodynamic Lubrication - Part I Fully Flooded Conditions", ASME Paper No. 74-LUB-31.

15. Archard, J. F. and Baglin, K. P., "Non-dimensional Presentation of Frictional Tractions in Elastohydrodynamic Lubrication - Part II Starved Conditions", ASME Paper No. 74-LUB-32.

16. Scheid, F., Theory and Problems of Numerical Analysis, Schaum's Outline Series, McGraw-Hill Book Co., 1968.

17. Sanborn, D. M., "An Experimental Investigation of the Elastohydrodynamic Lubrication of Point Contacts in Pure Sliding", Ph.D. Dissertation, University of Michigan, Ann Arbor, 1969.

18. Sanborn, D. M. and Winer, W. O., "Fluid Rheological Effects in Sliding Elastohydrodynamic Point Contacts with Transient Loading: 1 - Film Thickness", Trans. ASME, Journal of Lubrication Technology, Series F, Vol. 93, No. 2, 1973.

19. Sanborn, D. M. and Winer, W. O., "Fluid Rheological Effects in Sliding Elastohydrodynamic Point Contacts with Transient Loading: 2 - Traction", Trans. ASME, Journal of Lubrication Technology, Series F, Vol. 93, No. 3, 1973.

20. Novak, J. D., "An Experimental Investigation of the Combined Effects of Pressure, Temperature, and Shear Stress upon Viscosity", Ph.D. Dissertation, University of Michigan, Ann Arbor, 1968.

21. Roelands, C.J.A., "Correlational Aspects of the Viscosity-Temperature-Pressure Relationships of Lubricating Oils", Doctor Ingenieur Dissertation, Technische Hogeschool te Delft, 1966.

22. ASME, Pressure Viscosity Report, Vols. I and II, a report prepared by the ASME Research Committee on Lubrication, N. Y., 1953.

23. Johnson, K. L. and Roberts, A. D., "Rheology of Oil Films at High Contact Pressure", Nature, Vol. 240, No. 5383, 1972.

24. Sibley, L. B., "EHD Techniques and Application to the Design of Roller Bearings", Report AL71Q010, SKF Industries, Inc., Research Laboratory, 1971.

25. Lambelet, R. M., "Influence of the Cold Moving Surface Temperature, the Heat Conductivity of the Fluid, and of the Sliding Speed on the Shear Stress Distribution and on the Maximum Temperature in an Elastohydrodynamic Film", Report to Professor Ward O. Winer, Georgia Institute of Technology, Atlanta, 1973.

26. Carlson, S., Turchina, V., Jakobsen, J., Sanborn, D. M., and Winer, W. O., "Investigations of Lubricant Rheology as Applied to Elastohydrodynamic Lubrication", NASA Contact Report # 11-002-133, Georgia Institute of Technology, Atlanta, October, 1973.

27. Cheng, H. S., "Isothermal Elastohydrodynamic Theory for the Full Range of Pressure-Viscosity Coefficients", Trans. ASME, Journal of Lubrication Technology, Series F, Vol. 94, No. 1, 1972.

28. Jakobsen, J., Sanborn, D. M. and Winer, W. O., "Pressure-Viscosity Characteristics of a Series of Siloxane Fluids", Trans. ASME, Journal of Lubrication Technology, Series F, Vol. 96, No. 3, 1974.

29. Greenwood, J. A. and Kauzlarich, J. J., "Inlet Shear Heating in Elastohydrodynamic Lubrication", Trans. ASME, Journal of Lubrication Technology, Series F, Vol. 95, No. 4, 1973.

30. Walker, D. L., Sanborn, D. M. and Winer, W. O., "Molecular Degradation of Lubricants in Sliding Elastohydrodynamic Contacts", ASME Paper No. 74-LUB-35, 1974.

31. Carslaw, H. S. and Jaeger, J. C., Conduction of Heat in Solids, Oxford at Clarendon Press, 1962.

32. Jaeger, J. C., "Moving Sources of Heat and the Temperature at Sliding Contacts", Proc. Roy. Soc. of New South Wales, Vol. 76, 1942.

33. Cameron, A., The Principles of Lubrication, John Wiley and Sons, Inc., p. 235, New York, 1966.

34. Jakobsen, J., Sanborn, D. M. and Winer, W. O., "Investigations of the Rheology of a Series of Silicones as Related to Elastohydrodynamic Lubrication", A report prepared for Dow-Corning Corp., Midland, Mich. Georgia Institute of Technology, Atlanta, 1972.

35. Bohn, M., Carlson, S., Lee, D., Jakobsen, J., Sanborn, D. M., and Winer, W. O., "Investigations of Lubricant Rheology as Applied to Elastohydrodynamic Lubrication", NASA Contact Report # 11-002-133, Georgia Institute of Technology, Atlanta, June, 1972.